Dynamic NMR Study of the Interference between Cyclic Proton Exchange, Selfassociation and Hindered Rotation of Diphenylformamidine in Tetrahydrofuran

ARTICLE *in* BERICHTE DER BUNSENGESELLSCHAFT/PHYSICAL CHEMISTRY CHEMICAL PHYSICS · APRIL 1988

DOI: 10.1002/bbpc.198800112

3 AUTHORS, INCLUDING:

Hans-Heinrich Limbach
Freie Universität Berlin
333 PUBLICATIONS **8,943** CITATIONS

SEE PROFILE

Dynamic NMR Study of the Interference between Cyclic Proton Exchange, Selfassociation and Hindered Rotation of Diphenylformamidine in Tetrahydrofuran

Ludger Meschede, Detlef Gerritzen*), and Hans-Heinrich Limbach**)

Institut für Physikalische Chemie der Universität Freiburg i. Br., Albertstraße 21, D-7800 Freiburg, West Germany

Chemical Kinetics / Hydrogen Bonding / Isotope Effects / Proton Transfer / Spectroscopy, Nuclear Magnetic Resonance

The 90 MHz ^{1}H NMR spectra of ^{15}N,^{15}N′-dipentadeuterophenylformamidine (DPFA), a nitrogen analogue of formic acid, dissolved in tetrahydrofuran-d_8 (THF) have been measured as a function of concentration, deuterium fraction in the ^{1}H-^{15}N sites, and of temperature. The spectra show characteristic changes, from which thermodynamic and kinetic information on hindered rotation, hydrogen bond association and proton exchange of DPFA in THF are obtained by NMR lineshape analysis. DPFA forms two conformers A and B in THF, to which s-trans and s-cis structures have been assigned. At low concentrations both DPFA conformers are located in a hydrogen bond to the solvent molecules. However, as a result of the different structure, only A is able to selfassociate to any observable extent. This effect leads to concentration dependent A/B populations. Higher selfassociates or mixed AB associates are not observed. Whereas B is not able to exchange protons, A is subject to a very fast proton transfer. By measuring proton lifetimes as a function of concentration and of the deuterium fraction in the labile proton sites, it was established that two protons are transferred in every exchange process. Thermodynamic data of the association process obtained by the analysis of the chemical shifts, of the A/B populations and the proton lifetimes as a function of concentration agreed very well. These results are evidence that A forms only selfassociated hydrogen bonded dimers with a cyclic structure in which the double proton transfer takes place. The observation of a kinetic HH/HD isotope effect of 20 at 178 K establishes this transfer as the rate limiting step of the overall proton exchange. Rate constants of the double proton transfer in the cyclic dimer were obtained as a function of temperature from which an activation energy of about 19 kJ mol^{-1} was obtained. In addition, the rates of interconversion between the two conformers were determined as a function of temperature. Details of the reaction mechanism and differences to the related carboxylic acids are discussed. Thus, it is shown that dynamic NMR spectroscopy can be a useful tool for elucidating elementary steps of complex reaction networks.

1. Introduction

Dynamic NMR spectroscopy is a powerful tool for the study of hydrogen bonding and proton exchange in a number of different environments [1–5]. In the past years there has been a special interest in neutral multiple hydrogen transfer reactions, where at least two protons, hydrogen atoms or hydride ions are transferred between heavy atoms:

$$AH + XH^* \rightleftharpoons [AH, XH^*] \rightleftharpoons [AH^*, XH] \rightleftharpoons AH^* + XH \,. \quad (1)$$

Reactions of this kind have been studied not only in solution [6–16] but also in the solid state [17–22]. As models for the central exchange step in Eq. (1), the kinetics of intramolecular HH reactions in solution [23–28] and in the solid state [29–35] have also been followed by NMR methods. A particular feature of these reactions is that they can also be induced at cryogenic temperatures by light [36, 37], which might be of interest in optical storage devices [38]. In organic and biochemical systems these processes are related to bifunctional catalysis [39, 40] and biological activity [41–45]. In addition, these reactions are an old topic of theoretical chemistry [46–54] and of the theory of primary kinetic hydrogen/deuterium isotope effects [5, 7, 42, 49, 55–60].

There are several major problems in the study of intermolecular proton exchange reactions in solution. The first is the determination of the true rate constants of exchange within the reacting complex [AH, XH]. So far, only overall exchange rate constants have been obtained, which include terms arising from diffusion or from preequilibria between the separated reactants AH and XH and the reaction complex. The second problem is the determination of the number m of protons transferred in the rate limiting step, which is related to the structure of the reacting complex [AH, XH]. Information about m is not easy to obtain, even if the dependence of the exchange rates can be measured as a function of concentration. In principle, the measurement of so called "proton inventories" [41, 42] can be of assistance, where reaction rates are measured as a function of the deuterium fraction D in the mobile proton sites. This method has been successfully applied to the study of enzyme kinetics [41–45]. Such experiments can also help to solve the third problem, i.e. the determination of multiple kinetic isotope effects. So far, in order to extract m from a proton inventory, the validity of the "rule of the geometric mean" has been assumed, which states that for a double proton transfer

$$k^{HD} = (k^{HH} k^{DD})^{1/2}, \text{ i.e. } k^{HH}/k^{HD} = k^{HD}/k^{DD}. \quad (2)$$

This rule has been derived in terms of a combination of Bigeleisen's [58] equilibrium isotope effect and transition state theory [41, 42, 56–60]. In order to test Eq. (2) experimentally NMR proton inventory techniques [5, 7, 26] have recently been designed for the direct determination of k^{HH}, k^{HD}, and k^{DD} of inter- and intramolecular reactions according to Eq. (1): e.g. by a combination of ^{1}H and ^{2}H NMR measurements it was possible to measure such complete sets of kinetic isotope effects for the 1:1 and the 2:1 proton exchange between acetic acid (AH) and methanol (XH) in

*) Present Address Lonza AG, Visp, Switzerland.
**) Author for correspondence.

Ber. Bunsenges. Phys. Chem. *92*, 469–485 (1988)
0005–9021/88/0404–0469 $ 02.50/0

tetrahydrofuran [5, 7]. Large deviations from Eq. (2) were observed so far that replacement of the first H atom by D resulted in a stronger decrease of the rate constants than replacement of the second H atom by D, i.e. $k^{HH}/k^{HD} = 5.1$ and $k^{HD}/k^{DD} = 3$ at 298 K. Even larger deviations were found for the intramolecular HH migration in meso-tetraphenylporphin, where $k^{HH}/k^{HD} = 10$ and $k^{HD}/k^{DD} \approx 1$ [5]. These effects were interpreted in terms of tunneling and have been of use in the elucidation of kinetic results of enzyme reaction mechanisms [43, 44].

The scope of this study was to find an intermolecular multiple proton exchange system where it were possible to measure microscopic rate constants of the central exchange step in Eq. (1), including their multiple kinetic isotope effects. For this purpose we looked for a model which was able to form strong cyclic dimers, as do carboxylic acids. Double proton transfers in these compounds according to Scheme I are, however, extremely fast and energies of activation have only very recently been obtained for these reactions by solid state NMR T_1 measurements [18–22]. Kinetic HH/HD/DD isotope effects which could be a severe test for a proper theoretical description are, to date, still unknown for these processes. A second drawback in using carboxylic acids as model exchange systems is the fact that they do not contain nuclei with a suitable spin to enable easy probing of multiple kinetic isotope effects by NMR lineshape analysis. However, model compounds which fulfil these requirements are the amidines, which are the nitrogen analogues of the carboxylic acids (X = NR′ in Scheme I). Although the amidines are very old compounds [61], their physical and chemical properties are not very well known compared with the carboxylic acids. The amidine function has been shown to be of use in drugs [62]. IR studies of amidines [63, 64] have been interpreted with the formation of cyclic hydrogen bonded complexes with a structure similar to those of carboxylic acids. As a result, a double proton transfer according to Scheme I could take place in these complexes. A related double proton transfer in 7-azaindoles has been induced by light [37]. Kinetic information on the proton exchange behavior of amidines is, however, rare and incomplete so far that no rate laws nor kinetic isotope effects have as yet been reported. Halliday et al. [9] have made a lineshape analysis of the methyl group signals of neat dimethylformamidine (DMFA) and of DMFA dissolved in $CDCl_3$ at two concentrations. Surprisingly, the exchange rates were smaller in the sample with the higher concentration. Borisov et al. [10] have reported that N,N′-diphenylformamidine (DPFA) exists in tetrahydrofuran (THF) in an s-trans form A and an s-cis form B (Scheme II), which show different exchange characteristics. Since THF forms strong hydrogen bonds to proton donors leading to simplified rate laws for proton exchange [5, 7], we chose to perform a study of the latter system, results of which will be reported here. In order to avoid ^{14}N quadrupole effects and interference of the ^1H-^{15}N and the aromatic proton NMR signals, we actually studied ^{15}N,$^{15}N'$-dipentadeuterophenylformamidine (DPFA). The study of DPFA was especially appealing because of the possible comparison with an intramolecular HH transfer in the related tetraphenyloxalamidine (TPOA, Scheme III), which has been established recently [26].

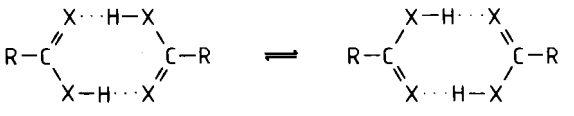

Scheme I

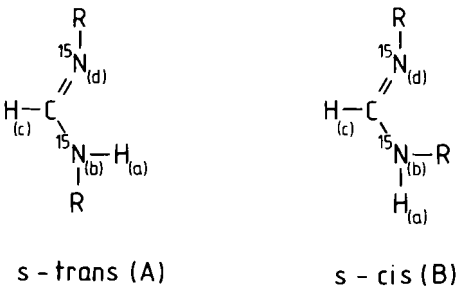

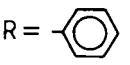

Scheme II

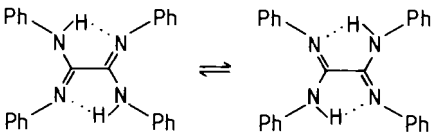

Scheme III

Following an experimental section, we describe the NMR lineshape theory used for the total lineshape analysis of the exchange broadened ^1H NMR spectra of DPFA in THF-d_8. Expressions are then derived, which relate experimental NMR parameters to the kinetic and thermodynamic data of the reactions of a four-spin system like DPFA in terms of a reaction model of proton exchange, hydrogen bond association and hindered rotation. We then present the temperature dependent ^1H NMR spectra of the system DPFA/THF-d_8, from which thermodynamic and kinetic information on the DPFA reactions in THF is obtained. From an ^1H NMR proton inventory the number of exchanging protons $m = 2$ is determined, as well as some kinetic HH/HD isotope effects and double proton transfer rate constants within the reacting cyclic DPFA dimer. Finally, the reaction mechanism evolving from the data is discussed.

2. Experimental

2.1. Synthesis of ^{15}N,$^{15}N'$-Dipentadeuterophenylformamidine (DPFA)

^{15}N,$^{15}N'$-dipentadeuterophenylformamidine (DPFA) was prepared from triethylorthoformate and C_6D_6-$^{15}NH_2$ by slightly modifying the method published for the unlabeled compound [61]. C_6D_6-$^{15}NH_2$ was synthesized as described previously [26]. DPFA was purified by recrystallization from n-heptane (Fp. 140 °C, Lit. 138 °C–141 °C [61]).

2.2. Preparation of Samples

The sealed NMR samples had to be prepared very carefully in order to exclude air and moisture or other impurities that might catalyse the proton exchange. For this purpose we used a vacuum line described previously [7, 14, 26]. Attached to the apparatus were glass vessels for solvent storage over drying agents, graduated

capillary tubes for volume measurements of liquids, and NMR tubes. Greaseless Teflon needle valve stopcocks were employed to separate these devices from the vacuum line. Anthracene/sodium-potassium alloy was employed as a drying agent for tetrahydrofuran-d_8 (THF), and molecular sieve (Merck, 3 Å), freshly activated in vacuo at 360°C with an electric oven for CH_3OL, L = H, D. The latter was used to prepare samples with a desired deuterium fraction D in the ^1H-^{15}N sites of DPFA. Before activation the molecular sieve was deuterated with H_2O/D_2O to the same degree. Weighted amounts of DPFA were placed in the NMR tube attached to the vacuum line and CH_3OL was condensed on the substrate, which dissolved. After evaporation, the same process was repeated twice. Repeated condensation and evaporation of THF on DPFA was then carried out to dry the compound. Finally, THF was transferred by successive evaporation and condensation into a graduated capillary tube thermostated to 298 K, and then transferred in defined amounts into the NMR tube. This was then sealed off. During this procedure the solutions were cooled to 77 K. The use of the graduated capillary tubes allowed us to prepare sealed samples of known total concentration C(298 K) of DPFA at 298 K. The values of C(298 K) were checked by recording the NMR spectra of all samples under the same experimental conditions and by comparing the absolute line intensities. Since the volume of THF is temperature dependent, the concentrations $C(T)$ at temperature T were calculated for each sample using the following equation [65]:

$$C(T)/C(298\ \mathrm{K}) = 1 + 9.26 \cdot 10^{-4} \cdot (298\text{-}T). \quad (3)$$

2.3. NMR Measurements

The NMR spectra were measured with a pulse FT NMR spectrometer, Bruker CXP 100, working at 90.02 MHz for protons. The sample temperatures were calibrated before and after the NMR measurements with a PT 100 resistance thermometer (Degussa) imbedded in an NMR tube, and are estimated accurate to about 0.5°C. The temperature stability during the measurements was, however, better than 0.2°C. The spectra were transferred from the Bruker Aspect 2000 minicomputer to a personal computer (Olivetti M 28), and then to the Univac 1108 computer of the Rechenzentrum der Universität Freiburg via a direct data line. Kinetic and thermodynamic parameters were obtained by simulation of the spectra as described below. Various experimental data were fitted to theoretical curves using a non-linear least squares fit program [66].

3. Evaluation of Thermodynamic and Kinetic Data

In this section we describe the formalism used for the evaluation of thermodynamic and kinetic data of different superposed exchange reactions of a nuclear spin system from its exchange broadened NMR spectra. The lineshape theory is based on the reaction network shown in Scheme IV, where each step gives rise to dynamic NMR linebroadening. First, we consider the presence of two interconverting isomers A and B with different nuclear spin hamiltonians. This interconversion proceeds without redistribution of nuclear spin functions corresponding to an intramolecular rearrangement. We let A be subject to intermolecular spin exchange, a process which does not change the hamiltonian but only redistributes the nuclear spin functions. Therefore, the products of spin exchange are labeled by an asterisk in Scheme IV. In the case of proton donors like DPFA this process corresponds to intermolecular proton exchange of isomer A. In addition, we consider the possibility that isomer A can exist in different rapidly exchanging species, e.g. monomers A_1, dimers A_2, or higher associates A_n, which correspond in the case of DPFA to different hydrogen bonded complexes. Thus, the spin hamiltonians are average hamiltoninas depending on temperature and on concentration. For B we only consider monomer species B_1 as indicated in Scheme IV. This then leads to the more complex reaction network shown in Scheme V where we assume that each species can form subspecies, e.g. free monomers A_{1f}, solvated monomers A_{1S}, solvated dimers A_{2S}, cyclic dimers A_{2C}, cyclic oligomers A_{nC} etc. We consider for isomer B only solvated monomers B_{1S} and free monomers B_{1f}. We allow spin exchange between molecules of A to take place in cyclic dimers or higher associates, i.e. $A_{2C} \cdots A_{nC}$. Note that throughout this paper a subspecies is defined as an element of a species and a species as an element of an isomer. Any element R, S ... will be called an "environment". Thus, in the following, K_{RS} will be the equilibrium and k_{RS} the rate constants of the reaction between the environments R and S. After describing the NMR lineshape theory we will derive expressions which relate these constants to observable static and dynamic NMR parameters.

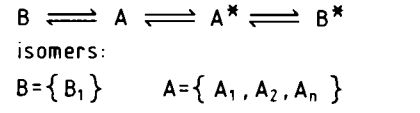

Scheme IV

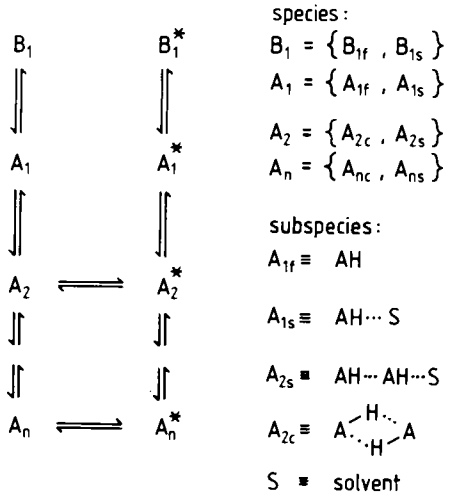

Scheme V

3.1. NMR Lineshape Theory of 4-Spin Systems in the Presence of Inter- and Intramolecular Exchange

The theory of NMR lineshapes of high order spin systems in the presence of intermolecular exchange has been described previously [11, 12, 67–69]. The theory was originally developed for continuous wave NMR spectroscopy under low power conditions. In modern pulse Fourier Transform NMR spectroscopy [70] used here, the theory can be conveniently summarized in the following way. During the free induction period following the preparation of single quantum coherence, the time dependence of the corresponding off diagonal elements of the density matrix ϱ of an ensemble of spins are governed by the master equation

$$\frac{d\varrho}{dt} = \mathcal{M}\varrho. \quad (4)$$

The dimension of the complex matrix $\mathscr{M}$ is equal to the number of transitions in the NMR spectrum of interest. Each transition m is characterized by the width Δ_m^{re} and the position Δ_m^{im}, where $\Lambda_m = \Lambda_m^{re} + i\Lambda_m^{im}$ is the mth complex eigenvalue of the matrix $\mathscr{M}$, calculated by diagonalization of $\mathscr{M}$ according to the transformation

$$\Lambda = C^{l}\mathscr{M}C^{r} . \tag{5}$$

The lineshape function is then conveniently written in the form

$$Y(\nu) \sim \sum_m \{[Q_m^{re}\Lambda_m^{re} - Q_m^{re}(\Delta_m^{im} - 2\pi\nu)]/ [(\Lambda_m^{re})^2 + (\Delta_m^{im} - 2\pi\nu)^2]\} , \tag{6}$$

where each transition m is further characterized by the complex intensity

$$Q_m = Q_m^{re} + iQ_m^{im} = Q_m = \left(\sum_k I_k^- C_{km}^r\right)\left(\sum_l \varrho_l(0) C_{lm}^l\right). \tag{7}$$

In Eq. (5) I_k^- are the elements of the lowering operator

$$I_k^- = I_{\mu_R \nu_R}^- = N_R^{-1}\langle \mu_R / I_R^- / \nu_R \rangle , \tag{8}$$

where μ_R and ν_R are the basis spin states and N_R the number of spin states in the environment R. $\varrho_l(0)$ represents the elements of the density matrix at the beginning of the acquisition at $t = 0$. In usual single pulse experiments these elements are given by

$$\varrho_k(0) = \varrho_{\mu_R \nu_R}(0) = p_R \langle \mu_R / I_R^- / \nu_R \rangle , \tag{9}$$

where p_R is the population of the environment R to which the spin states μ_R and ν_R are associated. The matrix $\mathscr{M}$, is set up as follows. $\mathscr{M}$ is given by [11, 12, 67–69]:

$$\mathscr{M} = -2\pi i(\mathscr{L} - \nu\varepsilon) + \mathscr{R} + \mathscr{X} . \tag{10}$$

In Eq. (10) ε is the unit matrix, ν the frequency, and $\mathscr{L}$ the Liouville operator with the elements

$$\mathscr{L}_{\mu_R \nu_R \kappa_S \lambda_S} = \mathscr{H}_{\mu_R \kappa_S}\delta_{\lambda_S \nu_R} - \mathscr{H}_{\lambda_S \nu_R}\delta_{\mu_R \kappa_S} . \tag{11}$$

$\mathscr{H}$ is the usual high resolution spin hamilton operator. Because of Eq. (11) $\mathscr{L}$ has a block structure, i.e. there are no off diagonal elements of $\mathscr{L}$ which connect different subsystems R. The high resolution hamilton operator $\mathscr{H}^R$ of the subsystem R is the sum of a Zeeman term and a term arising from scalar spin-spin interactions:

$$\mathscr{H}^R = \sum_i (\nu_{R_i} - \nu) I_{R_{zi}} + \sum_{i<j}\sum J_{R_{ij}} I_{R_i} I_{R_j} . \tag{12}$$

ν_{R_i} is the Larmor frequency of spin i, $J_{R_{ij}}$ the coupling constant between i and j, and I_i, I_{zi} the usual angular momentum operators of spin i in the subsystem R. $\mathscr{R}$ is the transverse part of the Redfield relaxation operator [69] in which we include artificial and apparative line broadening. Since we use the above lineshape theory only in the region where $|\mathscr{X}| \gg |\mathscr{R}|$ we retain here as usual only diagonal elements of $\mathscr{R}$, i.e. $\mathscr{R}_{ij} = -\delta_{ij}/T_{2i}^*$, where $1/T_{2i}^* = \pi(W_{oi})$ is the effective transverse relaxation time of the transition i. W_{oi} is the width of line i in the absence of exchange. The exchange operator $\mathscr{X}$ is a function of the type of exchange leading to the observed lineshape effects and of the pseudo first order rate constants i.e. the inverse correlation or lifetimes of the exchange. In contrast to intramolecular exchange processes, where the elements of $\mathscr{X}$ can be written down in a straightforward way, it is much more difficult to treat exchange processes where bonds are broken and formed. The most general exchange operator for intermolecular spin exchange has been derived previously [12] in a form, which avoids the assumption of reaction mechanism at the stage of evaluating the kinetic data.

In order to be more specific, let us consider a spin system containing four coupled $I = 1/2$ spins a to d, as is realized, for example, for DPFA (Scheme II). Let the spin system interconvert according to Scheme IV between two environments R = A, B. The basis spin functions can then be written as the product $\mu_R(a)\, i_R(b)\, j_R(c)\, k_R(d)$ of single spin functions which are either characterized by α or β because we consider here only $I = 1/2$ nuclei. According to Scheme IV the spin system can isomerise between the two isomers R, S = A, B. This process proceeds without redistribution of nuclear spins according to

$$\mu_R(a)\, i_R(b) j_R(c) k_R(d) \rightleftharpoons \mu_S(a)\, i_S(b) j_S(c) k_S(d). \tag{13}$$

From the NMR spectra the inverse lifetimes $\tau_{AB}^{-1}(iso)$ and $\tau_{BA}^{-1}(iso)$ of isomers A and B between two interconversions to B and to A can be obtained. $\tau_{RS}^{-1}(iso)$ is equal to the pseudo first order rate constant of interconversion from R to S. Intermolecular spin exchange of the first spin, whose spin function is characterized by a greek letter, results in a redistribution of the spin functions:

$$\begin{aligned}\mu_R(a)\, i_R(b) j_R(c) k_R(d) + \nu_S(a)\, l_S(b) m_S(c) n_S(d) \\ \rightleftharpoons \nu_R(a)\, k_R(b) j_R(c) i_R(d) \\ + \mu_S(a)\, n_S(b) m_S(c) l_S(d).\end{aligned} \tag{14}$$

In this equation we take into account that the intermolecular exchange of spin a is coupled to an intramolecular exchange of spins b and d as follows for DPFA on inspection of Schemes I and II. This process is characterized by the inverse lifetime $\tau_{AA}^{-1}(se)$ of spin a in isomer A between two successive spin exchange processes between A molecules according to Eq. (14). We neglect spin exchange from A to B and between B molecules, i.e. $\tau_{AB}^{-1}(se) = \tau_{BB}^{-1}(se) = 0$, and can therefore set $\tau_{AA}^{-1}(se) \equiv \tau_A^{-1}(se)$.

We can now write down in analogy to cases described previously [11, 12] the following complete exchange operator:

$$\begin{aligned}\mathscr{X}^{RS}{}_{\mu ijk,\nu lmn,\kappa opq,\lambda xyz} &= \tau_A^{-1}(se)\delta_{RA}\delta_{SA} \\ &\cdot \left[\frac{1}{2}\delta_{\mu\nu}\delta_{\kappa\lambda}\delta_{iq}\delta_{jp}\delta_{ko}\delta_{lz}\delta_{my}\delta_{nx} + \frac{1}{8}\delta_{\mu\kappa}\delta_{\nu\lambda}\delta_{il}\delta_{jm}\delta_{kn}\delta_{ox}\delta_{py}\delta_{qz}\right] \\ &+ \left[-\delta_{RS}\sum_{T\neq R}\tau_{RT}^{-1}(iso) + \tau_{RS}^{-1}(iso)(1-\delta_{RS}) - \tau_A^{-1}(se)\delta_{RA}\delta_{SA}\right] \\ &\cdot \delta_{\mu\kappa}\delta_{io}\delta_{jp}\delta_{kq}\delta_{\nu\lambda}\delta_{lx}\delta_{my}\delta_{nz} , \quad R,S = A,B.\end{aligned} \tag{15}$$

This equation takes the spin statistics into account, e.g. that there is a certain probability that the spin functions are not altered by the exchange when $\mu_R(a)\, i_R(b)\, j_R(c)\, k_R(d) = \nu_R(a)\, k_R(b)\, j_R(c)\, i_R(d)$ in Eq. (14). Thus, $\tau_A(se)$ is the average lifetime of an individual spin function between two successive intermolecular exchange events even if the spin function is not altered by this event. Since each four-spin system contributes 56 transitions to the lineshape, $\mathcal{M}$ has here the dimension 112. However, the size of $\mathcal{M}$ can be considerably reduced if one assumes that the spin systems are of first order. $\mathcal{L}$ is then diagonal and the 24 combination transitions can be omitted in $\mathcal{M}$. Each spin in the isomer R contributes then only 8 transitions to the ^{1}H NMR spectra. Since we have here two isomers R = A, B, $\mathcal{M}$ splits up in blocks of $16 \cdot 16$ submatrices for each spin. A general program of exchange broadened NMR spectra, which has been described previously [12] and which contains some subroutines of the program of Binsch [69], was used to calculate the ^{1}H NMR lineshape of DPFA. The program is written in such a way that it requires the Matrix $\mathcal{M}$ as input, calculated according to Eqs. (10)–(15). Input parameters are the pseudo first order rate constants τ_{RS}^{-1}(iso) and τ_A^{-1}(se), W_{oi}, chemical shifts ν_{R_i}, and coupling constants $J_{R_{ij}}$, i,j = a to d, R = A, B.

3.2. Evaluation of the Thermodynamic Data

In this section we derive appropriate expressions for the interpretation of the observable NMR parameters, e.g. the A/B populations and the chemical shifts of the exchanging proton in terms of the equilibrium constants shown in Scheme V.

3.2.1. Concentration Dependence of A/B Isomerism

If C_i is the concentration of the species i = A, B, the total concentration C is given by:

$$C = C_A + C_B \,. \tag{16}$$

If c_{A_i} and c_{B_i} are the concentrations of the subspecies A_i and B_i we can write down the following expressions:

$$C_A = c_{A_1} + 2c_{A_2} + \ldots + nc_{A_n} \,, \tag{17}$$

$$C_B = c_{B_1} + 2c_{B_2} + \ldots + nc_{B_n} \approx c_{B_1} \,. \tag{18}$$

According to Scheme V we neglect in Eq. (18) the formation of all selfassociates of B. For simplification we write τ_{RS}^{-1}(iso) $\equiv \tau_{RS}^{-1}$. If I is the observed A/B ratio, i.e.

$$I = C_A/C_B = \tau_{BA}^{-1}/\tau_{AB}^{-1} \tag{19}$$

it follows that for $C \rightarrow 0$

$$I_0 = k_{B_1A_1}/k_{A_1B_1} = K_{B_1A_1} \,. \tag{20}$$

$K_{B_1A_1}$ is the equilibrium constant of exchange between species B_1 and A_1. By combination of Eqs. (16)–(20) one can show that

$$C_A = CI/(I+1) \tag{21}$$

and that

$$c_{A_1} = CI_0/(I+1) \,. \tag{22}$$

Eq. (22) provides a unique measure of c_{A_1} which is generally very difficult to obtain. I depends on C in the following way. The concentrations of the remaining species in Scheme V are given by

$$c_{A_2} = c_{A_1}{}^2 K_{A_2}, \; K_{A_2} \equiv K_{A_1A_2} \,, \tag{23}$$

$$c_{A_n} = c_{A_1}^n K_{A_2} \prod_{n=3}^{m} K_{A_n}, K_{A_n} \equiv K_{A_{n-1}A_n} \,. \tag{24}$$

K_{A_2} and K_{A_n} are the equilibrium constants of dimerisation and of formation of A_n from A_{n-1}. By introducing Eqs. (22)–(24) into Eq. (16) and assuming that

$$K_{A_2A_3} \approx K_{A_3A_4} \approx \ldots \approx K_{A_{n-1}A_n} \equiv K_{A_n} \tag{25}$$

we obtain with Eq. (17)

$$C = C_A + C_B = c_{A_1}(1 + 1/I_0) + 2K_{A_2}c_{A_1}^2 + \sum_{n=3}^{m} nK_{A_2}K_{A_n}^{n-2}c_{A_1}^n \,. \tag{26}$$

Since each term in the sum is much smaller than 1, Eq. (26) converges and we obtain

$$C = c_{A_1}(1 + 1/I_0) - K_{A_2}c_{A_1}/K_{A_n} + K_{A_2}c_{A_1}/[(K_{A_n}(1 - K_{A_n}c_{A_1})^2] \,. \tag{27}$$

By combining Eqs. (22) and (27), we finally obtain the following relation between the observables I, I_0, and C:

$$C = [(I+1)/I_0K_{A_n}] \cdot [1 - \{I_0K_{A_2}/[K_{A_n}(I - I_0) + I_0K_{A_2}]\}^{1/2}] \,. \tag{28}$$

It can be shown that for $C \rightarrow 0$, $I \rightarrow I_0$ and for $C \rightarrow \infty$, $I \rightarrow \infty$. Eq. (28) can be recast into the form $I^3 + DI^2 + EI = 0$, where D and E are functions of C, I_0, K_{A_2}, and K_{A_n}. Analytical solutions of the cubic equation of the form

$$I = f(C) \tag{29}$$

can easily be found. For the case of $K_{A_n} \approx 0$ the cubic equation reduces to the quadratic form $I^2 + D'I + E' = 0$ with the solution:

$$I = \frac{1}{2}\,[I_0 - 1 + [(1 + I_0)^2 + 8K_{A_2}CI_0^2]^{1/2}], \tag{30}$$

or

$$C = \frac{1}{2}\,[(I+1)(I - I_0)/K_{A_2}I_0^2] \,. \tag{31}$$

By non-linear least squares fitting of the observed C vs. I values to Eq. (29), the different equilibrium constants contained in Eq. (28) can be obtained.

3.2.2. Concentration Dependence of Chemical Shifts

In the region of slow exchange between isomers A and B, the chemical shifts $\nu_{R_i} = \nu_{A_a}, \nu_{A_c}, \nu_{B_a}$ and ν_{B_c} are obtained by spectral simulation. The ν_{R_i} are the weighted averages over all hydrogen bonded species formed by R. The concentrations of the different hydrogen bonded species depend on the total concentration (Eqs. (26)–(28)) which leads to concentration dependent values of ν_{R_i}. Since we neglect selfassociation of B and mixed AB association, we can also neglect the dependence of the chemical shifts ν_{B_i} on concentration. Therefore, we are only concerned with the concentration dependence of ν_{A_i} for which one can write

$$\nu_{A_i} = 1/C_A \sum_l c_{A_l} \nu_{A_{li}} \quad \begin{matrix} i = \text{a to d (nuclei)}, \\ l = 1, n \text{ (species)}. \end{matrix} \tag{32}$$

Using the approximation of Eq. (25) we obtain by combination of Eqs. (21), (23), and (24):

$$\begin{aligned} \nu_{A_i} &= \nu_{A_{1i}} + 2(\nu_{A_{2i}} - \nu_{A_{1i}}) \frac{K_{A_2} C I_0^2}{I(I+1)} \\ &+ (\nu_{A_{ni}} - \nu_{A_{1i}}) \left[-\frac{K_{A_2} I_0}{K_{A_n} I} - \frac{2 K_{A_2} C I_0^2}{I(I+1)} \right. \\ &\left. + \frac{K_{A_2} I (I+1)^2}{K_{A_n} I [I+1-K_{A_n} C I_0]^2} \right], \quad C = C_A (I+1)/I. \end{aligned} \tag{33}$$

If A forms only dimers, i.e. if $K_{A_n} \approx 0$, the last three terms in Eq. (33) vanish, and in this case the relation between ν_{A_i} and C_A is given by

$$\begin{aligned} \nu_{A_i} &= \nu_{A_{1i}} + (\nu_{A_{2i}} - \nu_{A_{1i}}) \\ &\cdot \left[1 - \frac{1}{4 K_{A_2} C_A} [(8 K_{A_2} C_A + 1)^{1/2} - 1] \right]. \end{aligned} \tag{34}$$

It can be shown that for $C_A \to 0$ it follows that $\nu_{A_i} = \nu_{A_{1i}}$ and for $C_A \to \infty$ that $\nu_{A_i} = \nu_{A_{2i}}$. By combining Eqs. (29) and (33) analytical expressions for the function

$$\nu_{A_i} = f(C, I_0, K_{A_2}, K_{A_n}, \nu_{A_{1i}}, \nu_{A_{2i}}, \nu_{A_{ni}}) \tag{35}$$

can easily be obtained. Eq. (33) was incorporated in a general non-linear least squares fitting routine.

3.3. Evaluation of the Kinetic Data of the Reactions of DPFA in THF

In this section we derive expressions for the rate constants between the species in Scheme V as a function of the kinetic constants obtained by ^{1}H NMR lineshape analysis. In addition, we consider the case of multiple kinetic isotope effects of selfexchange reactions. In a previous study of measuring multiple kinetic isotope effects by NMR this case was not yet treated [7].

3.3.1. A/B Isomerism of DPFA

In this section we establish a relation between the pseudo first order A/B isomerisation rates $\tau_{AB}^{-1}(\text{iso}) \equiv \tau_{AB}^{-1}$ and $\tau_{BA}^{-1}(\text{iso}) \equiv \tau_{BA}^{-1}$ and the rate constant k_{ij} and k_{ji} of isomerisation, where $i = B_1$ and $j = A_1$ (Scheme V), via the following definition:

$$\tau_{AB}^{-1} \equiv -1/C_A (dC_A/dt)_{iso} = -1/C_A (dc_{A_1}/dt)_{iso} . \tag{36}$$

The last step follows from Eq. (11) and the assumption in Scheme V that rotational isomerism only takes place between A_1 and B_1. With the definition

$$k_{A_1B_1} \equiv -1/c_{A_1} (dc_{A_1}/dt)_{iso}$$

it follows that

$$\tau_{AB}^{-1} = (c_{A_1}/C_A) k_{A_1B_1} ,$$

and with Eqs. (21) and (22) that

$$\tau_{AB}^{-1} = k_{A_1B_1} (I_0/I) . \tag{37}$$

The dependence of τ_{AB}^{-1} on C can be expressed by combining of Eqs. (28) and (37). However, $k_{A_1B_1}$ can be directly obtained for each sample by inserting into Eq. (37) the known values of I and I_0.

3.3.2. Intermolecular Proton Exchange of DPFA

According to Eq. (15), the inverse lifetimes $\tau_A^{-1}(\text{se})$ of spin functions of environment A between two spin exchange processes according to Eq. (14) are measured by NMR lineshape analysis. In particular, in the case of monitoring proton exchange of DPFA by ^{1}H NMR lineshape analysis of the exchanging proton signals we can identify $\tau_A^{-1}(\text{se})$ with τ_{AH}^{-1}, the average lifetime of a protonated AH molecule between two exchange processes. In order to make the connection between τ_{AH}^{-1} and conventional rate constants let us first define the concentration of molecules in which a particular protonated A molecule can reside as

$$C'_A = \sum_n c_{A_n} . \tag{38}$$

In this expression A_n is counted only once in contrast to the total concentration of A molecules, $C_A = \sum_n n c_{A_n}$ as defined in Eq. (17) where A is considered formally as a monomer. Since all species and subspecies of A corresponding to the different hydrogen bonded environments are in fast exchange, we define the inverse lifetime τ_{AH}^{-1} by

$$\tau_{AH}^{-1} = -(1/C'_A)\, dC'_A/dt = -(1/C'_A) \sum_n (dc_{A_n}/dt) , \tag{39}$$

where Eq. (38) has been used. Since all species in the isomer A interconvert very rapidly within the NMR timescale, the rate limiting step of the overall proton transfer is the actual exchange within the species A_n. Let $k_{A_n} \equiv k_{A_nA_n}$ be the true rate constants of the exchange within this species. The average inverse proton lifetime of A is then given by the following expression:

$$\tau_{AH}^{-1} = -(1/C'_A) \sum_n k_{A_n} c_{A_n} . \tag{40}$$

By inserting Eq. (26) into Eq. (40) we obtain

$$\tau_{AH}^{-1} = -(1/C'_A) \sum_n k_{A_n} K_{A_2} K_{A_n}^{n-2} c_{A_1}^n \,. \tag{41}$$

If the exchange takes place only in one associate A_m it follows that

$$\tau_{AH}^{-1} = -(1/C'_A) k_{A_m} K_{A_2} K_{A_m}^{m-2} c_{A_1}^m \,. \tag{42}$$

If, in addition, only c_{A_1} and $c_{A_m} > 0$ it follows by combining Eq. (42) with Eqs. (21) and (27) that

$$\begin{aligned}\tau_{AH}^{-1} &= k_{A_m} K_{A_2} K_{A_m}^{m-2} \\ &\quad \cdot C^{m-1} I_0^m m[I(I+1)^{m-1}[I+I_0(m-1)]] \,,\end{aligned} \tag{43}$$

i.e.

$$\begin{aligned}\log(\tau_{AH}^{-1} I) &= (m-1)\log[C/(I+1)] \\ &\quad + \log k_{A_m} K_{A_2} K_{A_m}^{m-2} I_0^m m/[1+(I_0/I)(m-1)] \,.\end{aligned} \tag{44}$$

At low concentrations Eq. (44) reduces in good approximation to

$$\begin{aligned}\log(\tau_{AH}^{-1} I) &= (m-1)\log[C/(I+1)] \\ &\quad + \log k_{A_m} K_{A_2} K_{A_m}^{m-2} I_0^m \,.\end{aligned} \tag{45}$$

Thus, the observation that $\log(\tau_{AH}^{-1} I)$ is an approximately linear function of $[C/(I+1)]$ is evidence that the exchange takes place in one particular complex A_m. In addition, the number m can be obtained from the slope of Eq. (45). From the intercept of Eq. (45) the product $k_{A_m} K_{A_2} K_{A_m}^{m-2} I_0^m$ is obtained. Using Eq. (28) we can then recast Eq. (43) into the form:

$$\tau_{AH}^{-1} = f(C, I_0, k_{A_m}, K_{A_2}, K_{A_m}) \,.$$

For the simple case where only monomers and dimers are present and where the exchange takes place within the dimers we obtain

$$\tau_{AH}^{-1} = k_{A_2} F, \tag{46}$$

$$\begin{aligned}F = c_{A_2}/(c_{A_1} + c_{A_2}) &= (I - I_0)/(I + I_0) \\ &= \frac{4K_{A_2}C_A - [8K_{A_2}C_A + 1]^{1/2} + 1}{4K_{A_2}C_A + [8K_{A_2}C_A + 1]^{1/2} - 1} \,.\end{aligned} \tag{47}$$

Thus, τ_{AH}^{-1} is a linear function of F but a non linear function of C_A. Although at low concentrations τ_{AH}^{-1} increases linearly with C_A as expected for a second order rate law, it becomes equal to k_{A_2}, i.e. independent of C_A at high concentration indicating a first order rate law. This effect arises because at low C_A values all molecules are monomers but at infinitely high concentrations all molecules are located in the reacting dimers. Note, finally, that in the case of the multiple neutral intermolecular proton transfer reactions treated here, the number m of monomeric units in the cycling associate in which the proton transfer takes place is equal to the number of protons transferred.

3.4. NMR Proton Inventories for the Study of Multiple Proton Transfers and their Kinetic Isotope Effects

As shown previously [42], this number m of protons transferred during the chemical process can be obtained from so called proton inventories, where reaction rates are measured as a function of the deuterium fraction D in the labile proton sites. Particularly useful are NMR proton inventories [7], where inverse proton or deuteron lifetimes τ_{AH}^{-1} or τ_{AD}^{-1} can be measured by ^1H and ^2H NMR spectroscopy as a function of D. For a single proton transfer τ_{AH}^{-1} does not depend on D; for $m = 2$, τ_{AH}^{-1} should decrease linearly with increasing D [7], and for $m > 2$ one expects concave curved lines [7].

We deal here with the problem of a superposed selfexchange in cyclic dimers and trimers, a case which has not yet been included in our previous study [7]. The isotopic compositions of the dimers are expressed by the superscripts HH, HD, and DD and those of the trimers by HHH, HHD, HDD, and DDD. Since again all hydrogen bonded species interconvert rapidly, the inverse proton lifetimes are then given by the following equation:

$$\begin{aligned}\tau_{AH}^{-1} &= 1/C'_{AH}(dc_{A_2}^{HH}/dt + dc_{A_2}^{HD}/dt + dc_{A_3}^{HHH}/dt \\ &\quad + 2\,dc_{A_3}^{HHD}/dt + dc_{A_3}^{HDD}/dt)\end{aligned} \tag{48}$$

because in the case of selfexchange $dc_{A_3}^{HHD}/dt = dc_{A_3}^{HDH}/dt$ etc., i.e. $k_{A_3}^{HHD} = k_{A_3}^{HDH}$ etc. Note that the quantity C'_A in Eq. (39) has been replaced in Eq. (48) by the quantity C'_{AH} which indicates the concentration of molecules containing one or more protonated A molecules, which are labeled as AH. By inserting the appropriate rate laws we obtain:

$$\begin{aligned}\tau_{AH}^{-1} &= 1/C'_{AH}(k_{A_2}^{HH} c_{A_2}^{HH} + k_{A_2}^{HD} c_{A_2}^{HD} + k_{A_3}^{HHH} c_{A_3}^{HHH} \\ &\quad + 2k_{A_3}^{HHD} c_{A_3}^{HHD} + k_{A_3}^{HDD} c_{A_3}^{HDD}).\end{aligned} \tag{49}$$

In the absence of fractionation of isotopes between the different species i.e. if

$$C'_{AH} = (1-D)C'_A, c_{A_2}^{HH} = (1-D)^2 c_{A_2}, c_{A_2}^{HD} = D(1-D)c_{A_2} \text{ etc.}$$

we obtain

$$\begin{aligned}\tau_{AH}^{-1} &= [k_{A_2}^{HH}(1-D) + k_{A_2}^{HD} D](c_{A_2}/C'_A) \\ &\quad + [k_{A_3}^{HHH}(1-D)^2 + 2k_{A_3}^{HHD}(1-D)D + k_{A_3}^{HDD} D^2](c_{A_3}/C'_A).\end{aligned} \tag{50}$$

The quadratic terms in Eq. (50) disappear for a double proton transfer process. It is interesting to discuss for the latter case the results of Eq. (50). If $K_{A_1A_2}$ is very large, $c_{A_1} = 0$, $C_A = 2c_{A_2}$, and $C'_A = c_{A_2}$, and one obtains directly $k_{A_2}^{HH}$ and $k_{A_2}^{HD}$ from τ_{AH}^{-1} at $D = 0$ and $D = 1$. At $D = 0.5$ the lineshape function is determined by the constant $\tau_{AH}^{-1} = (1/2) \cdot (k_{A_2}^{HH} + k_{A_2}^{HD})$. Note, however, that this result applies only for a very rapid hydrogen bond exchange as mentioned above. If these processes were very slow, as for example in intramolecular double proton transfers, one would also obtain $k_{A_2}^{HH}$ and $k_{A_2}^{HD}$ at $D = 0$ and $D = 1$, but at $D = 0.5$ the lineshape would have to be described by a static superposition

of two independent lineshape functions, where the first function depends on $k^{HH}_{A_2}$ and the second on $k^{HD}_{A_2}$. For the case where $C'_A = c_{A_1} + c_{A_2}$ we obtain from Eq. (50) for the pure double proton transfer process

$$\tau_{AH}^{-1} \equiv \tau_{AH}^{-1}(C,D) = [k^{HH}_{A_2}(1-D) + k^{HD}_{A_2} D]\, F, \qquad F = (I-I_0)/(I+I_0). \tag{51}$$

The quantity τ_{AH}^{-1}/F is the inverse proton lifetime for the case I, i.e. $C \rightarrow \infty$. Thus, defining

$$\tau_{AH}^{-1}/F \equiv \tau_{AH}^{-1}(C \rightarrow \infty, D)$$

we obtain the simple equation

$$\tau_{AH}^{-1}(C \rightarrow \infty, D) = k^{HH}_{A_2}(1-D) + k^{HD}_{A_2} D. \tag{52}$$

The advantage of this equation is that τ_{AH}^{-1} values from samples with different concentrations C and deuterium fractions D can be directly compared and used to calculate the true rate constants in the exchanging dimers, $k^{HH}_{A_2}$ and $k^{HD}_{A_2}$. The kinetic HH/HD isotope effect of the double proton transfer can then be easily calculated from the linear decrease of

$$\tau_{AH}^{-1}(C \rightarrow \infty, D)/\tau_{AH}^{-1}(C \rightarrow \infty, D=0) = 1 - (1 - k^{HD}_{A_2}/k^{HH}_{A_2})D \tag{53}$$

with D.

4. Results

4.1. Description of the ^{1}H NMR Spectra of DPFA in THF-d_8

Typical experimental and calculated ^{1}H NMR spectra of a 0.004 M sample of DPFA in THF-d_8 are shown in Fig. 1 as a function of the temperature. We first discuss the spectrum at 152 K where we observe four multiplets which are assigned to the nuclei A_a, A_c, B_a, and B_c in Scheme II. As expected, A_a and A_c have the same integrated intensities, as well as B_a and B_c. The ratio $A_a/B_a \approx 3.5$ does not change very much with temperature. Evidence for the above assignment comes from the splitting pattern of the A_a and the B_a signals. The B_a signal is split into a doublet with a coupling constant of $J_{B_{ab}} = {}^1J_{^1H\text{-}^{15}N} = 91.8$ Hz, of which each component is further split into apparent triplets with coupling constants of $J_{B_{ad}} = {}^3J_{^1H\text{-}^{15}N} = 4.2$ Hz and $J_{B_{ac}} = 4.2$ Hz. Signal A_a is also split into a doublet with $J_{A_{ab}} = {}^1J_{^1H\text{-}^{15}N} = 92$ Hz; however, both doublet components are further split into a doublet with a coupling constant of $J_{A_{ac}} = 9.8$ Hz. The above values of $J_{A_{ac}}$ and $J_{B_{ac}}$ are further confirmed by lineshape simulation of the A_c and the B_c signals as described below. Note, however, that A_c and B_c are further split through coupling with their respective b and d spins. All coupling constants are listed in Table 1. Since the coupling constant $^3J_{H-N-C-H}$ is expected to be greater for conformer A as than for conformer B in analogy to previous cases [11], we can already confirm here the above assignment of the s-trans structure to conformer A and the s-cis structure to conformer B as shown in Scheme II in view of the observation that $J_{A_{ac}} > J_{B_{ac}}$.

As the temperature is raised to 189 K the components of signal A_a broaden because of proton exchange between A molecules, whereas the lineshape of the B_a signal is not altered, indicating that B is not subject to proton exchange. As the temperature is raised still further all lines broaden. This additional broadening is not a consequence of intermolecular proton transfer between A and B, which would only induce a coalescence of the ^{1}H-^{15}N signals A_a and B_a, but of a fast conformeric exchange between A and B due to hindered rotation. At room temperature only two signals of equal intensity are observed due to fast proton exchange and fast rotation between A and B. The coalesced A_c, B_c signal is slightly split into a triplet due to coupling with the two ^{15}N atoms. All splittings arising from the coupling of spin a with the other spins have disappeared because of the fast proton exchange.

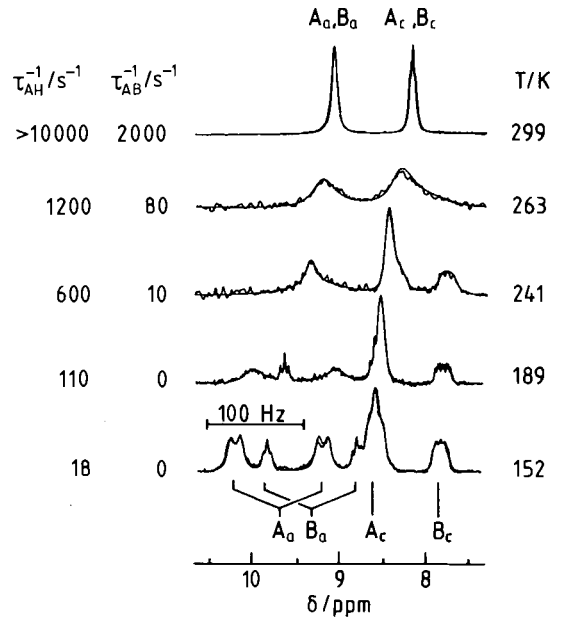

Fig. 1
Superposed experimental and calculated ^{1}H NMR 90.02 MHz spectra of ^{15}N,^{15}N′-diphenylformamidine-d_{10} in THF-d_8 for a concentration of 0.004 M as a function of the temperature. τ_{AB}^{-1}: forward rate constants of the hindered rotation between monomeric conformers A and B; A_a, B_a: ^{1}H-^{15}N sites; A_c, B_c: CH sites

Table 1
Experimental coupling constants $J_{R_{ij}}$, R = A, B, i = a, c, j = b to d, of the s-trans (A) and s-cis (B) conformers of ^{15}N,^{15}N′-DPFA-d_{10} in THF-d_8

$J_{A_{ij}}$/Hz	$J_{B_{ij}}$/Hz
$J_{ab} = 91.8 \pm 0.2$	$J_{ab} = 91.8 \pm 0.2$
$J_{ac} = 9.8 \pm 0.3$	$J_{ac} = 4.2 \pm 0.1$
$J_{ad} = 3.0 \pm 1.0$	$J_{ad} = 4.2 \pm 0.1$
$J_{cb} = 7.3 \pm 0.2$	$J_{cb} = 8.8 \pm 0.2$
$J_{cd} = 2.4 \pm 0.1$	$J_{cd} = 2.4 \pm 0.1$

Generally, the signals are averages of all possible hydrogen bonded states to which the molecules have access. Therefore, as the temperature is raised signals A_a and B_a shift to high field which is usual [4, 14] and which can be understood as follows. As will be shown later, at a concentration of 0.005 M selfassociation can be neglected and most molecules are monomeric, in particular in the solvated state $A_{1S} \equiv AH \cdots S$ and $B_{1S} \equiv BH \cdots S$, where S is the solvent. As temperature is increased the small amount of free monomers A_{1f} and B_{1f} is also increased, causing the observed upfield shifts of the average NH signals. However, in the evaluation of the kinetic and thermodynamic data we neglect the presence of A_{1f} and B_{1f}.

The fact that proton exchange between A molecules and rotational AB isomerism lead to two clearly different linebroadening mechanisms is demonstrated in Fig. 2, where ^{1}H NMR spectra of DPFA in THF-d_8 are shown as a function of concentration at 179 K. Whereas the lineshapes of signals B_a and B_c are independent of concentration, signal A_a in particular is subject to drastic changes with concentration. At low concentrations again we observe the

exchange broadened ^1H-^{15}N doublet of which both components coalesce at higher concentrations into a sharp singlet. The coalescence point is at about 0.03 M. The position of signal B_a is fairly constant as the concentration increases and indicates that B is in a hydrogen bonded state, i.e. in $B_{1S} \equiv BH \cdots S$. At low concentrations the position of signal A_a is not very different from the position of the signal B_a, indicating a similar hydrogen bonded state for A, i.e. $A_{1S} \equiv AH \cdots S$. By contrast, signal A_a shifts to lower field as the concentration increases, indicating an extensive selfassociation of conformer A at higher concentrations. Thus, it seems that there is a relation between the increased proton exchange rates and association of A as the concentration is increased. Note in Fig. 2 an additional important feature, i.e. the fact that the ratio $I = C_A/C_B$, where C_i is the total concentration of conformer i, increases with concentration. This is, as will be shown quantitatively later, also a consequence of the fact that A associates strongly, but not B. Similar behavior of a concentration dependent trans-cis isomerism due to excessive association of the trans conformer has been observed previously [10] for malonaldehydedianil. Thus, we have already obtained in a qualitative way evidence for the reaction model of Scheme V.

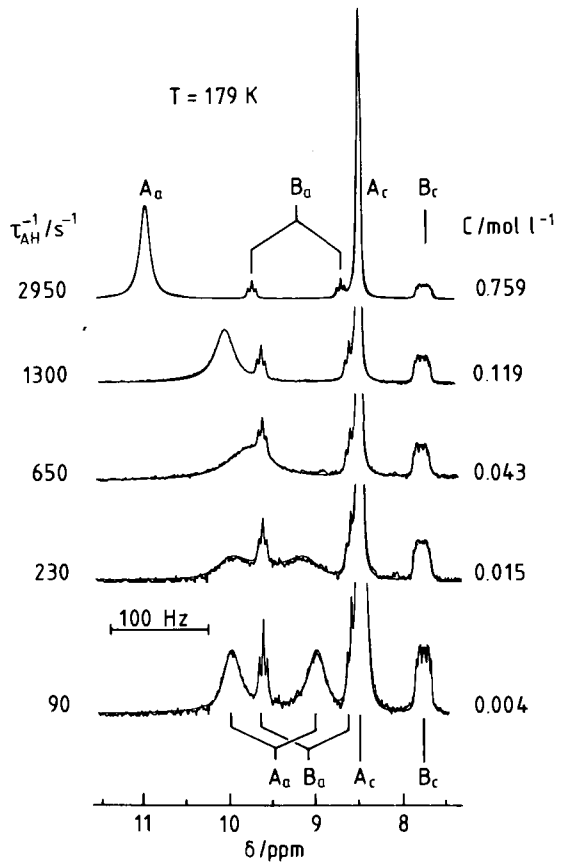

Fig. 2
Experimental and simulated ^1H NMR 90.02 MHz spectra of DPFA in THF-d_8 as a function of the concentration for a selected temperature of 179 K. τ_{AH}^{-1}: inverse NH proton lifetimes in A; A_a, B_a: ^1H-^{15}N sites; A_c, B_c: CH sites

4.2. Total Lineshape Analysis of the ^1H-NMR Spectra of DPFA in THF-d_8

The spectra of the type shown in Figs. 1 and 2 could be calculated as descibed in section 3. Parameters varied in the calculations were the chemical shifts of signals A_a, A_c, B_a, B_c, coupling constants, the linewidth W_0 in the absence of exchange, the mean proton lifetime τ_{AH} in conformer A, the s-trans/s-cis-population $I = C_A/C_B$ and the pseudo first order isomerisation rate constants τ_{AB}^{-1} and $\tau_{BA}^{-1} = \tau_{AB}^{-1} I$ of rotational isomerism. All simulation parameters are assembled in Tables 2–4. Unfortunately, the exchange broadened spectra do not contain information on all parameters at all temperatures. Therefore, we proceeded as follows.

Below 250 K, i.e. in the region of slow rotational isomerism the chemical shifts and I could be determined by total lineshape analysis. Since the chemical shifts were found to be linear functions of temperature, they were extrapolated to higher temperatures for the calculation of the spectra in the fast A/B exchange regime. In this regime above 250 K where signals A_a and B_a, as well as A_c and B_c have coalesced, I could be obtained from the positions of the average lines. For the determination of τ_{AB}^{-1} the values for the linewidth W_0 in the absence of isomerism were taken from the spectra of a reference sample of acetone in THF-d_8. At low temperatures this procedure may be not exact because of non negligible elements of the relaxation operator $\mathscr{R}$ in Eq. (8) [71]. However, because of the similar chemical structure of the two isomers A and B these elements were assumed to be similar for both isomers, and W_0 for the signals of A was, therefore, taken in this typical region from the linewidth of the corresponding B signals which are not affected by exchange broadening, as shown in Fig. 2. The only parameter which could not be resolved was the coupling constant $J_{A_{ad}}$ which affects the splitting of the A_a signal in the absence of proton exchange. Therefore, $J_{A_{ad}}$ was set to a value of 3 Hz in the lineshape calculations, which is the estimated limit above which we should have been able to resolve this splitting. Model calculations showed that the exact value of $J_{A_{ad}}$ is critical for the determination of the inverse proton lifetimes τ_{AH}^{-1} in A only in the regime where τ_{AH}^{-1} is smaller than 10 s^{-1}, i.e. a regime where we do not report τ_{AH}^{-1} values. The coupling constants $J_{A_{cb}}$ and $J_{A_{cd}}$ given in Table 1 could be extracted from the A_c signal at low temperatures of a 0.005 M probe with a deuterium fraction of $D = 95\%$ in the ^1H-^{15}N sites. However, during the simulation of the spectra above 250 K, we found that the lineshapes of signal A_c were consistent only with slightly smaller values of the order of $(J_{A_{cd}} + J_{A_{cd}})/2 \approx 3$ Hz. Since the A_c signal did not contain valuable information concerning the proton exchange rates, we did not study further whether these coupling constants were a function of concentration or of temperature.

All thermodynamic and kinetic parameters which are derived from the lineshape analysis given are assembled in Tables 3–6.

4.3. Thermodynamics of the s-Trans/s-Cis Isomerization and of Selfassociation of DPFA in THF

The equilibrium constants $K_{B_1A_1}$ of the hindered rotation between the monomers A_1 and B_1 were determined by simulation of the spectra of very dilute samples, where the s-trans/s-cis ratio $I = I_0 = K_{B_1A_1}$ (Table 3). The van't Hoff plot is shown in Fig. 3. The data can be represented by

$$K_{B_1A_1} = \exp[(1 \pm 1\,\mathrm{J\,mol^{-1}\,K^{-1}})/R] \cdot \exp[(-1.4 \pm 0.2\,\mathrm{kJ\,mol^{-1}})/RT], \quad 152\,\mathrm{K} < T < 294\,\mathrm{K}. \tag{54}$$

Thus, the enthalpy difference ΔH of 1.4 kJ mol^{-1} between B_1 and A_1 is very small, whereas the entropy difference is zero within the margin of error.

From the experimental dependence of $I = C_A/C_B$ on the concentration, additional thermodynamic information was obtained, as shown in Fig. 4 for a temperature of 179 K. A non-linear least squares fit of the data to Eq. (28) resulted in a value of $K_{A_n} \approx 0$, whereas $K_{B_1A_1} = 2.92 \pm 0.09$ and $K_{A_2} = 2.07 \pm 0.1$ l mol^{-1}. Thus, the data were equally well fitted in terms of Eq. (30) or of Eq. (31). Note that Eq. (31) contains only two variables, I_0 given by the intercept and K_{A_2} which describes the initial slope as well as the curvature of the non-linear function in Fig. 4.

In order to confirm independently the above observation that A is not able to form selfassociates A_n with $n > 2$, we have analyzed the chemical shifts ν of the A_a signal at 179 K as a function of the concentration. The experimental data were fitted to Eq. (33). The

Table 2
Experimental results of ^{1}H NMR 90.02 MHz measurements of ^{15}N,^{15}N′-DPFA-d_{10} in THF-d_8

S_N	T/K	$C(T)/M$	I_{cal}	I_{exp}	D	ν_{A_a}/Hz	ν_{B_a}/Hz	τ_{AH}^{-1}/s^{-1}	LB
1	175.3	0.762	6.49	7.6	0.0	1000.8	842.6	1600	3.5
1	176.2	0.761	6.43	6.9	0.0	1000.3	841.6	1800	3.2
1	178.0	0.760	6.29	6.4	0.0	998.8	838.6	1900	3.7
1	179.0	0.759	6.18	6.5	0.0	994.9	835.4	2950	3.0
1	183.5	0.757	5.86	6.9	0.0	992.0	836.7	2900	2.8
1	186.9	0.754	5.65	6.4	0.0	992.0	836.2	3300	2.5
1	188.6	0.753	5.53	6.2	0.0	985.2	833.9	3600	3.0
1	193.2	0.750	5.26	6.9	0.0	979.8	831.0	4600	2.7
1	194.9	0.749	5.17	6.4	0.0	979.3	830.4	5200	2.5
1	205.5	0.743	4.67	6.2	0.0	965.6	823.0	7300	3.0
2	164.2	0.419	6.10	5.9	0.0	990.3	844.0	850	3.2
2	171.4	0.417	5.53	5.6	0.0	981.7	840.1	1250	2.8
2	175.3	0.415	5.26	5.4	0.0	972.9	837.2	1600	2.5
2	176.2	0.415	5.22	5.3	0.0	972.4	835.7	1500	2.9
2	178.0	0.415	5.21	4.7	0.0	970.5	835.7	1750	3.0
2	179.0	0.414	5.03	5.3	0.0	969.6	835.4	2400	2.8
2	183.5	0.413	4.79	5.0	0.0	966.8	836.7	2400	2.5
2	186.9	0.412	4.64	5.5	0.0	960.2	829.9	2900	3.1
2	188.6	0.411	4.54	5.3	0.0	956.0	828.9	3200	3.0
2	193.2	0.409	4.34	4.8	0.0	951.0	826.0	4100	2.8
2	205.5	0.405	3.90	4.8	0.0	936.8	818.6	6500	3.0
3	158.9	0.282	5.80	4.3	0.0	975.3	842.5	610	2.5
3	171.4	0.280	4.92	3.4	0.0	957.7	835.7	1150	2.0
3	178.0	0.278	4.54	3.3	0.0	950.7	831.9	1700	2.9
3	179.0	0.277	4.47	4.3	0.0	944.9	831.2	2200	3.0
4	175.3	0.188	4.22	4.3	0.0	936.6	832.3	1080	3.2
4	176.0	0.188	4.19	4.0	0.0	937.4	831.6	1150	3.0
4	178.0	0.188	4.12	3.9	0.0	934.2	826.9	1300	3.5
4	179.0	0.188	4.06	4.2	0.0	928.6	829.5	1650	2.8
4	181.7	0.187	3.96	3.5	0.0	927.8	828.0	1600	3.5
4	187.5	0.186	3.76	3.7	0.0	917.9	823.6	2650	3.2
4	193.2	0.185	3.57	3.0	0.0	914.1	821.8	2800	3.0
4	198.0	0.184	3.45	2.9	0.0	906.4	818.3	3900	2.9
5	175.3	0.172	4.15	4.0	0.0	933.5	831.5	1050	3.5
5	176.0	0.171	4.10	3.8	0.0	927.8	830.0	1150	3.0
5	178.0	0.171	4.03	3.7	0.0	928.4	826.9	1250	2.8
5	179.0	0.171	3.97	4.1	0.0	925.1	829.3	1600	2.6
5	181.7	0.171	3.88	4.0	0.0	922.9	826.7	1850	3.0
5	187.5	0.170	3.69	3.2	0.0	915.2	824.0	2350	3.3
5	193.2	0.169	3.51	3.3	0.0	911.9	821.8	2500	3.1
5	212.3	0.166	3.07	3.2	0.0	891.0	811.6	4800	2.9
6	162.5	0.121	4.39	3.7	0.0	931.1	835.1	550	3.0
6	165.5	0.120	4.23	3.6	0.0	934.4	835.5	610	2.9
6	175.1	0.119	3.84	3.7	0.0	919.2	830.5	980	3.1
6	178.0	0.119	3.74	3.7	0.0	913.8	828.9	1000	3.2
6	179.0	0.119	3.69	3.8	0.0	912.1	828.2	1300	3.3
6	181.7	0.119	3.61	2.9	0.0	910.0	825.8	1550	2.9
6	185.1	0.118	3.51	2.9	0.0	907.2	825.0	1700	3.0
6	187.5	0.118	3.44	2.5	0.0	903.5	823.1	1750	2.8
6	191.3	0.117	3.34	3.2	0.0	898.9	821.0	2400	2.8
6	198.0	0.117	3.19	2.8	0.0	892.2	816.9	2750	3.5
7	171.4	0.095	3.83	3.7	0.0	914.5	831.0	680	2.9
7	178.0	0.095	3.60	3.2	0.0	907.5	828.4	900	3.2
7	179.0	0.094	3.55	2.9	0.0	905.6	827.5	1350	2.7
8	176.0	0.092	3.63	4.0	0.0	906.2	828.9	820	2.8
8	178.0	0.092	3.58	3.3	0.0	903.4	827.5	870	2.9
8	179.0	0.092	3.54	3.7	0.0	902.6	827.5	1070	3.2
8	187.5	0.092	3.32	3.2	0.0	895.0	823.6	1290	3.0
8	193.2	0.091	3.17	2.8	0.0	890.0	820.5	1690	3.2
8	198.0	0.091	3.09	2.8	0.0	881.5	816.5	2700	3.0
8	209.4	0.090	2.87	2.4	0.0	872.6	810.1	3550	3.1
9	158.9	0.044	3.83	4.7	0.0	902.1	836.1	250	3.3
9	175.3	0.043	3.33	4.9	0.0	883.4	827.5	460	2.9
9	179.0	0.043	3.22	3.4	0.0	885.9	826.8	650	2.7
9	187.5	0.043	3.05	4.1	0.0	867.3	820.4	740	3.1
9	193.2	0.043	2.94	3.5	0.0	877.0	821.4	800	2.9
9	198.8	0.042	2.85	2.7	0.0	869.5	815.6	1300	3.1
9	209.4	0.042	2.70	2.3	0.0	859.7	809.5	2000	2.9
9	212.3	0.042	2.66	2.3	0.0	861.2	810.7	2100	3.3
9	220.2	0.042	2.57	2.1	0.0	854.5	805.0	2900	2.9

Table 2 *(Continued)*

S_N	T/K	$C(T)/M$	I_{cal}	I_{exp}	D	ν_{A_a}/Hz	ν_{B_a}/Hz	τ_{AH}^{-1}/s^{-1}	LB
10	164.2	0.015	3.35	4.0	0.0	876.0	833.7	170	3.2
10	171.4	0.015	3.18	3.3	0.0	874.0	829.9	220	2.9
10	179.0	0.015	3.03	3.1	0.0	866.3	825.9	230	3.1
10	186.9	0.014	2.89	2.8	0.0	862.8	822.5	270	2.9
10	194.9	0.014	2.77	2.4	0.0	855.0	817.6	400	3.1
10	205.5	0.014	2.63	2.5	0.0	854.0	812.3	650	3.0
11	151.0	0.005	3.57	3.3	0.0	872.6	839.1	12	2.9
11	152.3	0.005	3.53	3.3	0.0	872.6	838.7	18	3.1
11	175.4	0.005	3.08	2.9	0.0	861.2	827.0	70	3.0
11	175.4	0.005	3.08	2.9	0.0	861.2	827.0	70	3.1
11	176.2	0.005	3.00	3.1	0.0	860.6	826.0	80	3.0
11	179.0	0.005	2.95	3.0	0.0	859.2	825.8	90	2.9
11	188.6	0.005	2.80	2.9	0.0	856.2	820.9	110	3.2
11	215.0	0.004	2.50	2.4	0.0	843.8	804.3	400	3.5
11	236.8	0.004	2.31	2.3	0.0	834.1	795.2	550	3.5
11	241.1	0.004	2.28	2.2	0.0	832.2	793.1	600	3.8
11	256.1	0.004	2.19	2.2	0.0	825.7	785.6	700	4.0
11	262.7	0.004	2.15	2.1	0.0	822.6	782.0	1200	3.6
11	281.7	0.004	2.06	2.1	0.0	807.8	771.3	1550	3.8
11	294.0	0.004	2.00	2.0	0.0	798.2	764.4	4000	3.5
12	175.3	0.223	4.40	3.8	0.90	937.3	832.4	200	3.0
12	178.0	0.223	4.29	3.6	0.90	936.5	831.8	230	3.2
13	162.6	0.120	4.38	3.6	0.93	929.5	839.0	60	3.0
13	165.5	0.120	4.30	3.4	0.93	923.0	835.0	90	3.1
13	171.4	0.120	4.09	2.7	0.93	916.7	832.2	105	2.9
13	176.0	0.119	3.80	3.2	0.93	910.3	829.4	140	3.2
13	178.0	0.119	3.74	3.3	0.93	911.0	828.8	130	3.0
13	181.7	0.118	3.61	2.7	0.93	905.0	827.0	140	2.9
13	185.1	0.118	3.41	2.9	0.93	900.8	824.7	180	3.2
13	199.3	0.117	3.10	2.4	0.93	880.8	818.1	340	2.7
13	209.4	0.116	2.96	2.6	0.93	873.2	811.2	540	2.9
13	209.9	0.116	2.96	3.6	0.93	870.8	810.0	580	2.9
13	220.2	0.115	2.79	3.1	0.93	866.1	805.5	1150	3.0
13	230.1	0.114	2.59	2.8	0.93	861.8	801.2	1550	3.2
14	171.4	0.107	3.91	3.2	0.85	913.8	832.0	115	3.3
14	178.0	0.107	3.60	2.6	0.85	903.5	826.2	150	2.9
14	199.3	0.105	3.11	2.6	0.85	882.8	816.1	390	3.2
14	220.2	0.103	2.67	2.2	0.85	867.4	805.1	1000	2.8
14	230.1	0.102	2.66	1.6	0.85	860.5	801.8	2100	3.2
15	171.4	0.121	4.01	3.0	0.48	918.5	831.9	440	2.9
15	178.0	0.120	3.85	2.6	0.48	912.7	828.9	570	3.1
16	176.0	0.095	3.65	3.2	0.50	903.4	828.9	380	3.2
16	178.0	0.095	3.60	2.8	0.50	904.0	827.5	490	3.1
16	181.7	0.094	3.56	3.1	0.50	897.7	824.9	720	2.9
16	187.5	0.094	3.39	2.8	0.50	891.6	821.8	860	3.0
16	209.4	0.092	2.88	2.3	0.50	872.6	810.8	2200	2.7

S_N: number of sample, T: absolute temperature, $C(T)$: total concentration at given temperatures, I_{exp}: experimental, I_{cal}: calculated values of the ratio of A and B conformers according to Eq. (30), D: deuterium fraction in the NH sites, ν_{A_a}, ν_{B_a}: NH chemical shifts of A and B (TMS), τ_{AH}^{-1}: inverse NH proton lifetimes of A, LB: sum of artificial and apparative line broadening.

parameter I_0 was taken from Fig. 4 and was not varied. Again we obtained $K_{A_n} \approx 0$ and $K_{A_2} = 1.83 \pm 0.2$ l mol^{-1} at 179 K, which corresponds well with the value obtained from Fig. 4 and with the form of Eq. (34). Therefore, all data were interpreted in terms of Eq. (34). Fig. 5 shows the chemical shifts of the A_a signal as a function of concentration of A, C_A. In order to obtain K_{A_2} as a function of temperature we proceeded as follows. We measured carefully the chemical shifts for each sample as a function of temperature and obtained linear relations for $\nu = f(T)$. Least squares fitting of the data allowed us to calculate the chemical shifts for all samples at given temperatures with a very high accuracy. The ν values were then fitted to Eq. (34) as shown in Fig. 5. The corresponding van't Hoff plot is shown in Fig. 6, where the straight line is given by:

$$K_{A_2} = \exp[(-21.6 \pm 0.5\,\mathrm{J\,mol^{-1}\,K^{-1}})/RT] \cdot \exp[4.8 \pm 0.3\,\mathrm{kJ\,mol^{-1}})/RT]\,\mathrm{l\,mol^{-1}}, \quad 150\,\mathrm{K} < T < 200\,\mathrm{K}. \tag{55}$$

Thus, the formation of cyclic dimers is exothermic, but the entropy decreases as expected.

4.4. Kinetics of the Hindered Rotation between the Monomeric Conformers A_1 and B_1 of DPFA in THF

Fig. 7 shows the Arrhenius diagram of the experimental rate constants $k_{A_1B_1}$ of the rotational isomerism between the monomeric species A_1 and B_1. The data stem from the sample of Fig. 1 where $C = 0.005$ mol l^{-1} and from a sample where $C = 0.373$ mol l^{-1}. The simulated τ_{AB}^{-1} values were multiplied by the experimental factor I/I_0 according to Eq. (37) in order to calculate $k_{A_1B_1}$, although this factor is close to 1 at $C < 0.01$ mol l^{-1}. We obtain by linear least squares fit of log $k_{A_1B_1}$ vs. $1/T$:

$$k_{A_1B_1} = 10^{13.8 \pm 0.5} \exp[(-59.7 \pm 0.5\,\mathrm{kJ\,mol^{-1}})/RT]\,\mathrm{s^{-1}}, \quad 215\,\mathrm{K} < T < 298\,\mathrm{K}. \tag{56}$$

Table 3
Experimental equilibrium- and rate constants of A/B rotational isomerism

S_N	T/K	$C(T)$/M	$K_{B_1A_1}$	$k_{A_1B_1}/s^{-1}$	LB
2	215.2	0.402	–	0	3.5
2	239.2	0.393	–	8	3.5
2	241.1	0.393	–	8	3.8
2	246.6	0.391	–	13	4.0
2	255.7	0.388	–	16	3.5
2	257.2	0.387	–	50	3.2
2	259.8	0.386	–	54	3.0
2	262.7	0.385	–	70	3.3
2	264.2	0.384	–	115	3.5
2	298.7	0.373	–	2840	3.8
11	152.3	0.005	3.3	–	3.1
11	175.4	0.005	2.9	–	3.0
11	176.2	0.005	3.1	–	3.0
11	179.0	0.005	3.0	–	2.9
11	188.6	0.005	2.9	–	3.2
11	215.0	0.004	2.4	0	3.5
11	236.8	0.004	2.3	8	3.5
11	241.1	0.004	2.2	10	3.8
11	256.1	0.004	2.2	50	4.0
11	262.7	0.004	2.1	80	3.8
11	281.7	0.004	2.1	550	3.5
11	294.0	0.004	2.0	2800	3.5

S_N: number of sample, T: absolute temperature. Explanation of the other symbols see text and Table 2.

Table 4
Experimental results of the ^1H NMR measurements of DPFA in THF at $T = 179$ K

S_N	$C(T)$/M	I_{exp}	$C_A(T)$/M	ν_{A_a}/Hz	$\tau_{AH}^{-1}/^{-1}$
1	0.759	6.5	0.658	994.1	2950
2	0.414	5.3	0.348	969.6	2400
3	0.277	4.3	0.255	944.9	2200
4	0.188	4.2	0.152	928.6	1650
5	0.171	4.1	0.137	925.1	1600
6	0.119	3.75	0.094	912.1	1300
7	0.094	3.7	0.074	905.6	1350
8	0.092	3.7	0.072	902.6	1070
9	0.043	3.4	0.033	885.9	650
10	0.015	3.1	0.011	866.3	230
11	0.005	3.0	0.003	859.2	110

S_N: number of sample, C: total concentration, I: experimental values of the A/B ratio, C_A: concentration of s-trans form A, τ_{AH}^{-1}: inverse NH lifetimes, ν_{A_a}: shifts of the NH signals a of isomer A.

Table 5
Results of the chemical shift analysis of the NH signal ν_{A_a} according to Eq. (33). I_0 values are not fitted, but calculated from Fig. 4

T/K	$\nu_{A_{1a}}$/Hz	$\nu_{A_{2a}}$/Hz	$I_0 = K_{B_1A_1}$	K_{A_2}/ 1 mol^{-1}
160.0	864.2	1131.8	3.264	2.59
165.0	862.5	1127.9	3.160	2.40
170.0	860.7	1124.4	3.064	2.21
175.0	858.9	1120.4	2.977	2.02
179.0	857.9	1121.5	2.928	1.93
180.0	857.0	1120.8	2.897	1.83
185.0	855.2	1118.4	2.823	1.65
187.5	854.0	1118.8	2.781	1.55
190.0	853.2	1119.7	2.754	1.47

T: absolute temperature, ν_{A_i} ($i = 1_a, 2_a$): NH chemical shifts of monomeric A_1 and cyclic dimeric species A_2, $K_{B_1A_1}$, K_{A_2}: equilibrium constants of rotational isomerism and of dimerization of A.

Table 6
Calculated rate constants of HH- and HD transfers in cyclic dimeric complexes of DFPA according to Eq. (51)

T/K	$k_{A_2}^{HH}/s^{-1}$	$k_{A_2}^{HD}/s^{-1}$	K_{A_2}/ 1 mol^{-1}
151.0	940	–	3.29
152.3	1570	–	3.21
158.9	2750	–	2.75
162.5	3540	152	2.54
164.2	4615	–	2.45
165.5	4170	243	2.38
171.4	6240	305	2.11
175.3	6450	428	1.96
176.0	6900	536	1.94
176.2	7570	–	1.93
178.0	7600	500	1.88
179.0	11000	–	1.82
181.7	11678*	1080	1.74
183.5	8870	–	1.70
185.1	15600	870	1.65
186.9	12860	–	1.60
187.5	16620	1100	1.59
188.6	14820	–	1.56
191.3	24320	–	1.51
193.2	18870	–	1.45
194.9	21900	–	1.41
198.0	32210	–	1.36
198.8	23750	–	1.35
199.3	32000*	2150	1.33
205.5	37710	–	1.21
209.4	58950	5250	1.15
209.9	54130*	3548	1.14
212.3	57315	–	1.11
215.0	99600	–	1.07
220.2	103570	8430	1.01
230.1	128878	20893	0.90

T: absolute temperature, D: deuterium fraction in the ^1H-^{15}N sites. For explanation of symbols see text. *: calculated according to Eq. (57), K_{A_2} values calculated according to Eq. (55).

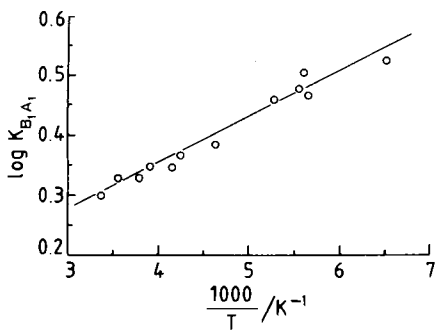

Fig. 3
Van't Hoff diagram of the s-trans/s-cis isomerization of DPFA in THF. The equilibrium constants $K_{B_1A_1}$ were determined by lineshape analysis of the spectra partly shown in Fig. 1

4.5. NMR Proton Inventory of DPFA in THF

In order to get an idea of how many protons are involved in the intermolecular proton exchange of DPFA in THF and in order to obtain information on the nature of rate limiting step as well as on kinetic isotope effects, we have measured proton exchange rates in DPFA/THF samples as a function of the deuterium fraction D in the NH sites. These measurements were done before establishing the rate law of proton exchange described in the next paragraph.

Typical NMR lineshapes of the ^1H-^{15}N signals A_a and B_a are shown in Fig. 8 for a total concentration of about 0.1 M and a temperature of 178 K as a function of the deuterium fraction D.

Only the A_a signal and the left triplet component of the B_a signal were simulated. The proton lifetimes τ_{AH}^{-1} decrease with increasing D, which is proof of a multiple proton transfer process according to Eq. (52). Further data are listed in Table 2. For a proton inventory according to Eq. (53), the $\tau_{AH}^{-1}(C \to \infty, D)/\tau_{AH}^{-1}(C \to \infty, D = 0)$ values were plotted in Fig. 9 as a function of the deuterium fraction D. As expected for a double proton transfer process with $m = 2$ in terms of Eq. (53), a linear decrease was obtained within the margin of error. By linear least squares fitting of the data to Eq. (53), a kinetic HH/HD isotope effect of 22 at 178 K was obtained. This analysis was carried out at several temperatures.

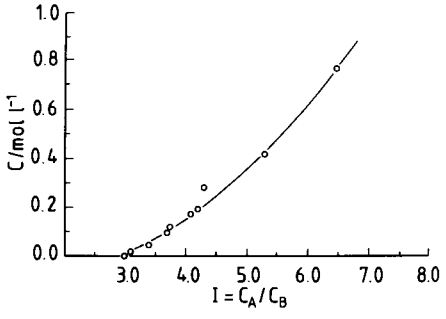

Fig. 4
Dependence of the ratio $I = C_A/C_B$ of the total concentration $C = C_A + C_B$ at 179 K. The value of I for $C \to 0$ is given by $I_0 = c_{A_1}/c_{B_1} = K_{B_1A_1}$. The solid line was calculated by non-linear least squares fit of the data to Eq. (31)

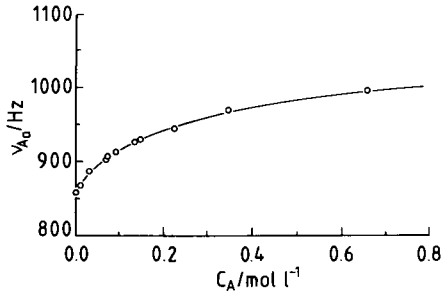

Fig. 5
Experimental and calculated chemical shifts ν_{A_a} of the ^1H-^{15}N signal A_a of DPFA in THF as a function of the concentration C_A of the conformer A at 179 K. C_A was determined from the known values of I and C. The solid line was calculated by non-linear least squares fit of the data to Eq. (34)

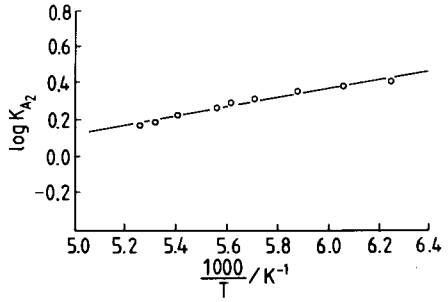

Fig. 6
Van't Hoff diagram of the dimerization of the s-trans form A of DPFA in THF. The K_{A_2} values were obtained by analysis of the chemical shifts ν_{A_a} of the A_a signal. For further explanation see text

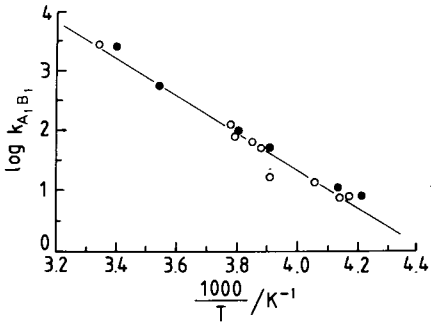

Fig. 7
Rate constants $k_{A_1B_1}$ of the hindered rotation between monomeric molecules A_1 and B_1 as a function of the temperature for selected samples. ○: $C_{298K} = 0.005$ M; ●: $C_{298K} = 0.373$ M

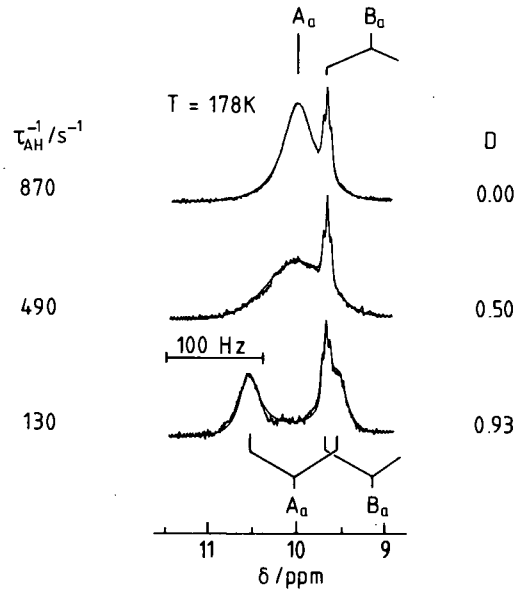

Fig. 8
Superposition of the experimental and calculated ^1H NMR 90.02 MHz spectra of DPFA in THF-d_8. Only the ^1H-^{15}N signal A_a of conformer A is shown as a function of the deuterium fraction D in the ^1H-^{15}N sites at a concentration of 0.1 M at 178 K. Note also the left triplet component of the signal B_a

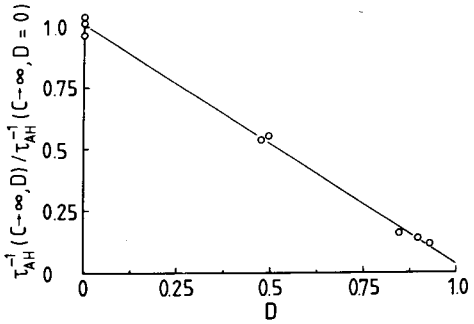

Fig. 9
Proton inventory plot for proton exchange of the s-trans conformer A of DPFA in THF-d_8 according to Eq. (53) at 178 K. $\tau_{AH}^{-1}(C \to \infty, D)/\tau_{AH}^{-1}(C \to \infty, D = 0)$ is the relative inverse proton lifetimes extrapolated to high concentrations and D the deuterium fraction D in the mobile ^1H-^{15}N sites

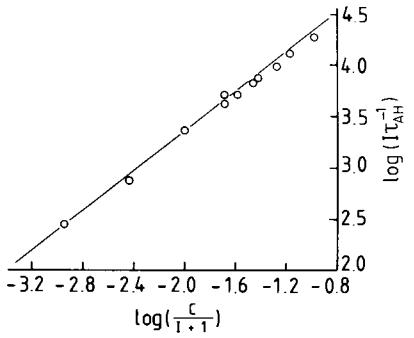

Fig. 10
Experimental and calculated values of log ($\tau_{AH}^{-1}I$) as a function of log ($C/(I+1)$) at 179 K according to Eq. (45). For further explanation see text

4.6. Kinetics of Proton Exchange of DPFA in THF

In order to confirm the value of $m = 2$ independently we plotted in Fig. 10 according to Eq. (45) the values of log ($\tau_{AH}^{-1}I$) vs. log ($C/(I+1)$). τ_{AH} is the experimental proton lifetime in the s-trans conformer A, I the s-trans/s-cis ratio and C the total concentration. I was calculated from the known value of K_{A_2} and I_0 according to Eq. (30) (see Table 2). At low concentrations we obtain a straight line with a slope of 0.98 ± 0.03. Thus, Eq. (45) is valid and m = 1.98 ± 0.02, i.e. 2 molecules of A participate in the exchange process. This corresponds very well with the results of the proton inventory.

We then plotted the experimental τ_{AH}^{-1} values at 179 K as a function of $F = (I-I_0)/(I+I_0)$, where I was calculated according to Eq. (30) from the known value of K_{A_2} (Table 2). As predicted by Eq. (46) and as shown in Fig. 11, we found a linear dependence of τ_{AH}^{-1} as a function of F, with an intercept of zero. Thus, the assumption inherent in Eq. (46), i.e. that only one type of dimer is formed in which the exchange takes place, seems to be well fulfilled. A value for the rate constant k_{A_2} in the dimer of $k_{A_2} = 10700\ s^{-1}$ was obtained from the slope of the solid line in Fig. 11. A similar result was obtained if the experimental I values (Table 2) were used. Thus, the dimers monitored by analysis of the chemical shifts and of the s-trans/s-cis populations should be of the same type as those monitored by the kinetic measurements of proton exchange. In other words, the more complex reaction scheme in Scheme V should be valid. Since in this case the dimerization constants K_{A_2} in Eqs. (23), (27), and in Eqs. (45), (47) are identical and since we knew the value of k_{A_2}, we were able to calculate the inverse proton lifetimes τ_{AH}^{-1} as a function of the concentration C_A according to Eq. (46). The result is shown as a solid line in Fig. 12 together with the experimental values. The agreement between the experimental and the calculated data is very satisfactory. The very interesting non-linear character of the function τ_{AH}^{-1} vs. C is particularly well reproduced. This curvature, which is very sensitive to the value of K_{A_2}, arises from the following effect: at low concentrations the pseudo-first order rate constants τ_{AH}^{-1} are linear in C_A, i.e. a second order rate law $v = C_A/\tau_{AH} \sim C_A^2$ prevails because two A molecules are needed for the exchange to take place. However, at higher concentrations a kind of saturation occurs and the τ_{AH}^{-1} values seem to become independent of C_A, i.e. $v = C_A/\tau_{AH} \sim C_A$. This is expected if all A molecules are located in the subspecies in which the exchange of the two proton takes place, i.e. if the cyclic dimers of Scheme I are dominant. Thus, as a result of the good agreement of the experimental and calculated values in Fig. 12, we have obtained evidence for the validity of the above assumption that the chemical shift and the s-trans/s-cis population analysis and the analysis of the kinetic data monitor the formation of the same dimers A_2, in particular the cyclic dimer A_{2C} from the solvated monomer $A_{1S} \equiv AH\cdots S$. In other words, there is a very high probability that $K_{A_2} \equiv K_{A_1A_2}$ is essentially equal to $K_{A_{1S}A_{2C}}$, the equilibrium constant of formation of the cyclic dimers from the solvated monomers, and that k_{A_2} is directly the rate constant of double proton transfer in the cyclic dimers.

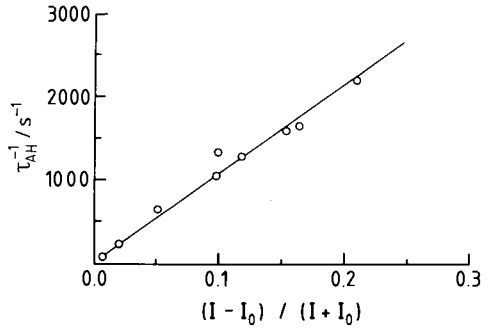

Fig. 11
Experimental and calculated inverse ^1H-^{15}N proton lifetimes τ_{AH}^{-1} in conformer A as a function of $(I-I_0)/(I+I_0)$ at 179 K. The values of I were calculated according to Eq. (30). The solid line was fitted to the experimental points in from which the slope of k_{A_2} = 10700 cm^{-1} is obtained using Eq. (46). For further explanation see text

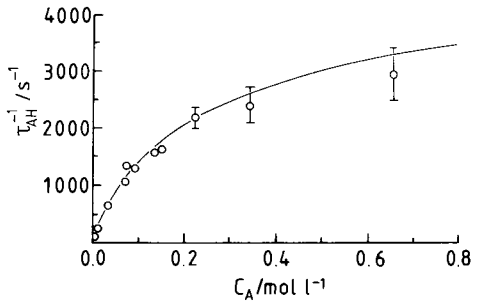

Fig. 12
Experimental and calculated inverse ^1H-^{15}N proton lifetimes τ_{AH}^{-1} in conformer A as a function of the concentration C_A of conformer A at 179 K. The solid line was calculated using Eq. (46) from the known values of the constants $K_{B_1A_1}$, K_{A_2}, and k_{A_2}

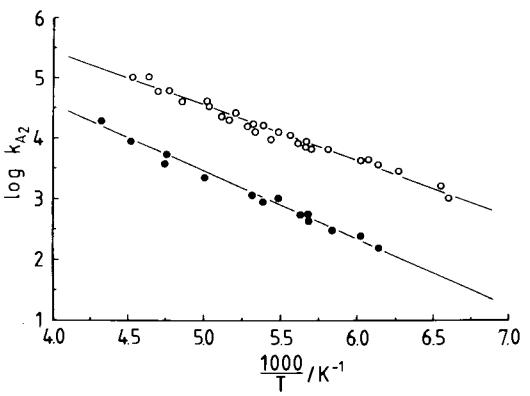

Fig. 13
Arrhenius diagram of the experimental and calculated data of the intermolecular HH- and HD migrations in cyclic dimers of the s-trans conformer A of DPFA in THF-d_8

The analysis of Figs. 11 and 12 was then also performed at other temperatures. Values of k_{A_2} are given in Table 6. From the Arrhenius diagram shown in Fig. 13 we calculate:

$$k_{A_2}^{HH} = 10^{9.0\pm0.3}\exp[(-17.2\pm0.5\,kJ\,mol^{-1})/RT]\,s^{-1}, \quad 151\,K < T < 230\,K. \tag{57}$$

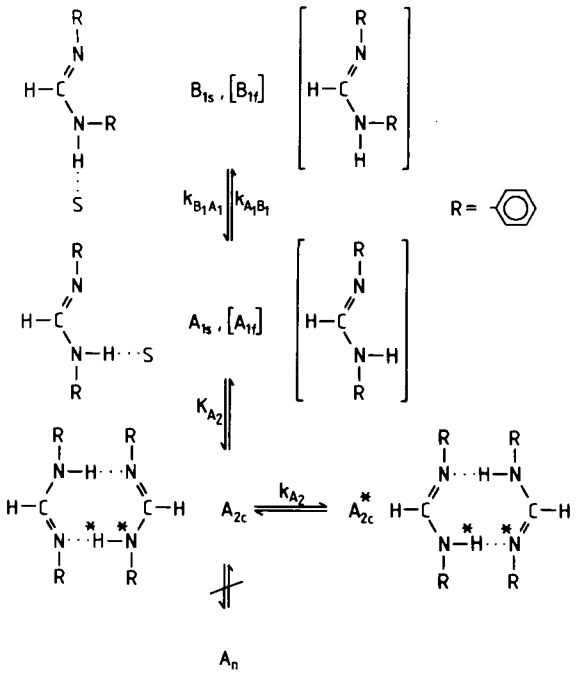

Fig. 14
Exchange processes of DPFA in THF as identified by NMR. K_i and k_i are equilibrium and rate constants obtained by lineshape analysis. [ ] represent possible intermediates present in minor concentrations. S ≡ solvent

In a similar way, neglecting equilibrium isotope effects we obtain:

$$k_{A_2}^{HD} = 10^{8.9 \pm 1.0} \exp[(-21.2 \pm 1.5\,\mathrm{kJ\,mol^{-1}})/RT]\,\mathrm{s^{-1}}, \quad 162\,\mathrm{K} < T < 230\,\mathrm{K}. \tag{58}$$

By extrapolation we obtain $(k^{HH}/k^{HD})_{298\,K} \approx 5.7$. Note that the errors given in Eqs. (57) and (58) are of a statistical nature and do not include systematic errors or errors due to assumptions.

5. Discussion

As shown above, by analysis of the ^{1}H NMR spectra of diphenylformamidine (DPFA), a wealth of thermodynamic and kinetic information on hindered rotation, hydrogen bond association and proton exchange of DPFA in THF is obtained by NMR lineshape analysis. From this analysis we can draw the following detailed picture of molecular events in the system DPFA/THF, as shown in Fig. 14. DPFA exists in THF in an s-trans conformer A and an s-cis conformer B. Almost all B molecules form a hydrogen bond with the solvent, S, i.e. are located in the subspecies B_{1S}. At low concentrations A is located in a similar state A_{1S}. A_{1S} and B_{1S} interconvert with measurable rotational exchange rates $k_{A_1B_1}$ which can be interpreted in terms of $k_{A_{1S}B_{1S}}$, given by Eq. (56). The preexponential factor has a value of $10^{13}-10^{14}$ s^{-1} which is typical for intramolecular rearrangements. It is possible that the rotation proceeds via the free monomers A_{1f} and B_{1f}. In this case, part of the high energy of activation stems from the breaking of the hydrogen bond to the solvent. The energy and entropy difference between A_{1S} and B_{1S} is small, as indicated by Eq. (54). At higher concentrations A is subject to selfassociation. However, in contrast to the carboxylic acids [14], no solvated linear dimers $A_{2S} \equiv AH\cdots AH\cdots S$ or oligomers A_n are observed, but only cyclic dimers A_{2C}. In these dimers a fast cooperative double proton transfer takes place. However, the observation of a kinetic HH/HD isotope effect clearly establishes this double proton transfer as the rate limiting step of the proton exchange, the interconversion of the different hydrogen bonded species and subspecies being very fast, as is indicated by the observation of only averaged NMR signals for all species and subspecies. The number of transferred protons $m = 2$ has been established by performing a proton inventory, and additionally, by analysis of the complex experimental rate law. The fact that only the conformer A is subject to proton exchange and selfassociation but not conformer B can be easily seen by a breakdown of the ^{1}H-^{15}N splitting and the low field shift of signal A_a in Fig. 2 as concentration is increased: the position and the ^{1}H-^{15}N splitting pattern of signal B_a in Fig. 1 is unaffected by concentration changes. From an analysis of the ^{1}H-^{15}N chemical shifts and of the A/B populations as a function of concentration, the equilibrium constant K_{A_2} could be obtained. The values obtained by both methods agreed within the margin of error. Thus, K_{A_2} could be interpreted as the equilibrium constant $K_{A_{1S}A_{2C}}$ of the formation of the cyclic dimers from the solvated monomers. Its temperature dependence is given in Eq. (55). There is a slight decrease in energy, indicating that a hydrogen bond in the cyclic complex is stronger than a hydrogen bond between A and the solvent. By contrast, there is a decrease in entropy as expected for the formation of a cyclic dimer. The consistency of this interpretation was further confirmed by the observation that the inverse proton lifetimes in A, τ_{AH}^{-1}, depend in a non-linear way on the concentration, as shown in Fig. 12. Thus, we find a second order rate law at low concentrations because two DPFA molecules are involved in the exchange. However, at higher concentrations the rate law changes gradually to first order because at very high concentrations all A molecules are in the subspecies A_{2C}. This finding is in a way similar to the case of enzyme reactions, where the rate law also changes in the region where all enzymes are loaded with the substrate. Here we can regard one of the exchanging DPFA molecules as the "substrate" and the other as the "enzyme" which transports a proton from one location in the substrate to another. These observations might also explain the kinetics of proton exchange observed previously for the related triazenes R−NH−N=N−R [8], where, depending on the substituent R, first or second order rate laws were obtained. Different substituents R lead to different values of the dimerisation constants K_{A_2}. Small K_{A_2} values lead to second, large K_{A_2} values to first order kinetics as expressed by Eq. (50). Thus, the decrease of the proton exchange rates with increasing concentration found by Halliday et al. [9] for dimethylformamidine in $CDCl_3$ might reflect a decrease of K_{A_2} due to formation of higher linear associates.

Since K_{A_2} could be determined as a function of temperature, we were able to obtain values of the exchange rate constants k_{A_2} in the exchanging cyclic dimers. So far, rate constants of intermolecular proton transfer reactions have, to our knowledge, always been affected by terms arising from diffusion or from preequilibria between the molecules

in non-reacting and reacting hydrogen bonded states. Thus, we are now able to compare k_{A_2} with the corresponding solid state values which are, unfortunately, not yet known up to date or with values for intramolecular double proton transfer reactions in related molecules, e.g. in tetraphenyloxalamidine (TPOA) shown in Scheme III. According to Eq. (57), the DPFA reaction is characterized by a surprisingly small barrier for the proton transfer, about 2.5 times smaller than the barrier for the TPOA tautomerism [26]. By extrapolation we obtain a room temperature ratio of $k_{DPFA}/k_{TPOA} \approx 500$. This difference is understandable because TPOA is not able to form strong linear hydrogen bonds like DPFA. However, the energy of activation of the double proton transfer in cyclic hydrogen bonded DPFA dimers is much higher than the corresponding value for the double proton transfer in carboxylic acids [18–22]. At present, we can only speculate as to whether this effect is due to the replacement of oxygen by nitrogen, to a different geometry, or to the attached phenyl groups in DPFA. Possibly the double proton transfer in DPFA dimers is coupled to a phenyl group reorientation.

The presence of the phenyl groups in DPFA could also be the origin for the different association behaviour of DPFA in THF as compared to carboxylic acids. Note that in a previous study [14] we found that acetic acid forms in THF many more dimers of the type $A_{2S} \equiv AH \cdots AH \cdots S$ than cyclic dimers. One might argue that steric hindrance between the phenyl groups is not in favor of the formation of A_{2S}. On the other hand, molecular models show that steric hindrance between the phenyl groups probably also results in an angle between the phenyl groups and the amidine plane. Unfortunately, no X-ray structure of diarylamidines is available up to date.

The question arises whether the proton transfer is better described in terms of conventional transition state theory by reaction over the barrier, or whether tunneling plays a dominant role. This question cannot be answered at present in view of the small temperature range for which $k_{A_2}^{HD}$ values could be obtained. The preexponential factor and the activation energy of the HD process given in Eq. (58) are, therefore, preliminary and might be subject to a larger error as indicated by the statistical errors given in Eq. (58). Tunneling contributions may be detected by measuring the complete kinetic HH/HD/DD isotope effects of the reaction. In the future, we will try to obtain such sets of kinetic HH/HD/DD isotope effects for the formamidine reaction, now where the nature of this transfer has now been established.

We conclude that it is possible to obtain very detailed information on the elementary steps of complex reaction networks in solution by NMR. Especially it is possible in favorable cases to obtain directly rate constants in reaction complexes which are not affected by diffusion or preequilibria.

We thank the Deutsche Forschungsgemeinschaft, Bonn-Bad Godesberg and the Fonds der Chemischen Industrie Frankfurt for financial support. The calculations were done on the Univac 1108 computer of the Rechenzentrum der Universität Freiburg i. Br.

References

[1] E. Grunwald, in: "Proton Transfer", E. Caldin and V. Gold, eds., Chapman and Hall, p. 103, London 1975.
[2] "The Hydrogen Bond", P. Schuster, G. Zundel, and C. Sandorfy, eds., North Holland Publ. Comp., Amsterdam 1976.
[3] G. S. Denisov, S. F. Bureiko, N. S. Golubev, and K. G. Tokhadse, in: "Molecular Inter actions", H. Ratajczak and W. J. Orville-Thomas, eds., Wiley, Vol. 2, chapter 2 p. 107, Chichester 1980.
(4) H. H. Limbach, " The Use of NMR Spectroscopy in the Study of Hydrogen Bonding in Solution", in: "Aggregation Processes", J. Gormally, E. Wyn-Jones, eds., chapter 16, Elsevier, Amsterdam 1983.
[5] H. H. Limbach, J. Hennig, D. Gerritzen, and H. Rumpel, Faraday Discuss. Chem. Soc. *74*, 229 (1982).
[6] D. Gerritzen and H. H. Limbach, Ber. Bunsenges. Phys. Chem. *85*, 527 (1981).
[7] D. Gerritzen and H. H. Limbach, J. Am. Chem. Soc. *106*, 869 (1984).
[8] L. Lunazzi and G. Panciera, J. Chem. Soc. Perkin 2, *1980*, 52.
[9] J. D. Halliday, E. A. Symons, and P. E. Bindner, Can. J. Chem. *56*, 1470 (1978).
[10] E. V. Borisov, D. N. Kratsov, A. S. Peregudov, and E. I. Fedin, Izv. Akad. Nauk SSSR, Ser. Khim. *1980*, 2151.
[11] H. H. Limbach and W. Seiffert, Ber. Bunsenges. Phys. Chem. *78*, 641 (1974).
[12] H. H. Limbach, J. Magn. Reson. *36*, 287 (1979).
[13] H. H. Limbach and W. Seiffert, J. Am. Chem. Soc. *102*, 538 (1980).
[14] D. Gerritzen and H. H. Limbach, J. Phys. Chem. *84*, 799 (1980).
[15] V. A. Bren, V. A. Chernoivanov, L. E. Konstantinovskii, L. E. Nivorozhkin, Y. A. Zhdanov, and V. I. Minkin, Dokl. Akad. Nauk SSSR *251*, 1129 (1980).
[16] A. N. Nesmeyanov, V. N. Babin, E. B. Zavelovitch, and N. S. Kochetkova, Chem. Phys. Lett. *37*, 184 (1976).
[17] A. Baldy, J. Elguero, R. Faure, M. Pierrot, and E. J. Vincent, J. Am. Chem. Soc. *107*, 5290 (1985).
[18] S. Nagagoka, T. Terao, F. Imashiro, A. Saika, N. Hirota, and S. Hayashi, Chem. Phys. Lett. *80*, 580 (1981); J. Chem. Phys. *79*, 4694 (1983).
[19] B. H. Meier, F. Graf, and R. R. Ernst, J. Chem. Phys. *76*, 767 (1982).
[20] F. Graf, R. Meyer, T. K. Ha, and R. R. Ernst, J. Chem. Phys. *75*, 2914 (1981).
[21] S. Benz, U. Haeberlen, and J. Tegenfeldt, J. Magn. Reson. *66*, 125 (1986).
[22] S. Idziak and N. Pislewski, Chem. Phys. *111*, 439 (1987).
[23] C. B. Storm and Y. Teklu, J. Am. Chem. Soc. *94*, 1745 (1974); Ann. N.Y. Acad. Sci. *206*, 631 (1973).
[24] H. H. Limbach, H. Hennig, and J. Stulz, J. Chem. Phys. *78*, 5432 (1983); J. Hennig and H. H. Limbach, J. Am. Chem. Soc. *106*, 292 (1984); J. Hennig and H. H. Limbach, J. Magn. Reson. *49*, 322 (1984).
[25] M. Schlabach, B. Wehrle, H. H. Limbach, E. Bunnenberg, A. Knierzinger, A. Shu, B. R. Tolf, and C. Djerassi, J. Am. Chem. Soc. *108*, 3856 (1986).
[26] G. Otting, H. Rumpel, L. Meschede, G. Scherer, and H. H. Limbach, Ber. Bunsenges. Phys. Chem. *90*, 1122 (1986).
[27] F. Graf, Chem. Phys. Lett. *62*, 291 (1979).
[28] H. H. Limbach and D. Gerritzen, J. Chem. Soc. Faraday Discuss. *74*, 279 (1982).
[29] H. H. Limbach, H. Hennig, R. D. Kendrick, and C. S. Yannoni, J. Am. Chem. Soc. *106*, 4059 (1984).
[30] H. H. Limbach, D. Gerritzen, H. Rumpel, B. Wehrle, G. Otting, H. Zimmermann, R. D. Kendrick, and C. S. Yannoni, in: „Photoreaktive Festkörper", H. Sixl, J. Friedrich, and C. Bräuchle, eds., p. 19–43, M. Wahl Verlag, Karlsruhe 1985.
[31] R. D. Kendrick, S. Friedrich, B. Wehrle, H. H. Limbach, and C. S. Yannoni, J. Magn. Reson. *65*, 159 (1985).
[32] H. H. Limbach, B. Wehrle, H. Zimmermann, R. D. Kendrick, and C. S. Yannoni, J. Am. Chem. Soc. *109*, 929 (1987).
[33] H. H. Limbach, B. Wehrle, H. Zimmermann, R. D. Kendrick, and C. S. Yannoni, Angew. Chem. Int. Ed. Eng. *26*, 247 (1987).
[34] B. Wehrle, H. H. Limbach, M. Köcher, O. Ermer, and E. Vogel, Angew. Chem. Int. Ed. Eng. *26*, 934 (1987).

[35] B. Wehrle, H. Zimmermann, and H. H. Limbach, J. Am. Chem. Soc., in press.
[36] S. Völker and J. H. van der Waals, Mol. Phys. *32*, 1703 (1976).
[37] C. A. Taylor, M. A. El. Bayoumi, and M. Kasha, Proc. Natl. Acad. Sci. U.S.A. *63*, 253 (1969); K. Tokumura, Y. Watanabe, M. Udagawa, and M. Itoh, J. Am. Chem. Soc. *109*, 1346 (1987) and references cited therein.
[38] J. Friedrich and D. Haarer, Angew. Chem. Int. Ed. Engl. *23*, 113 (1984).
[39] C. G. Swain and J. F. Brown, J. Am. Chem. Soc. *74*, 2534 (1952); *74*, 2538 (1952); M. Ek and P. Ahlberg, Chem. Scr. *16*, 62 (1980); K. A. Engdahl, H. Bivehed, P. Ahlberg, and W. H. Saunders, Jr., J. Chem. Soc. D: *1982*, 423.
[40] O. Bensaude, M. Chevrier, and J. E. Dubois, J. Am. Chem. Soc. *101*, 2423 (1979).
[41] J. P. Elrod, R. D. Gandour, J. L. Hogg, M. Kise, G. M. Maggiora, R. L. Schowen, and K. S. Venkatasubban, Faraday Symp. Chem. Soc. *10*, 145 (1975).
[42] R. D. Gandour and R. L. Schowen, "Transition States of Biochemical Processes", Plenum Press, New York 1978.
[43] J. D. Hermes and W. W. Cleland, J. Am. Chem. Soc. *106*, 7263 (1984).
[44] J. D. Hermes, S. W. Morrical, M. H. O'Leary, and W. W. Cleland, Biochemistry *23*, 5479 (1984).
[45] J. G. Belasco, W. J. Albery, and J. R. Knowles, Biochemistry *25*, 2529 (1986); ibid. *25*, 2552 (1986).
[46] A. Sarai, Chem. Phys. Lett. *83*, 50 (1981); J. Chem. Phys. *76*, 5554 (1982); ibid. *80*, 5341 (1984).
[47] G. I. Bersuker and V. Z. Polinger, Chem. Phys. *86*, 57 (1984); W. Siebrand, T. A. Wildman, and M. Z. Zgierski, J. Am. Chem. Soc. *106*, 4083 (1984); ibid. *106*, 4089 (1984).
[48] M. J. S. Dewar, J. Mol. Struct. (Theochem) *124*, 183 (1985).
[49] R. P. Bell, "The Tunnel Effect in Chemistry", Chapman and Hall, London 1980.
[50] J. Brickmann and H. Zimmermann, Ber. Bunsenges. Phys. Chem. *70*, 157 (1966); ibid. *70*, 521 (1966); ibid. *71*, 160 (1967); J. Brickmann and H. Zimmermann, J. Chem. Phys. *50*, 1608 (1969).
[51] E. Ady and J. Brickmann, Chem. Phys. Lett. *11*, 302 (1971).
[52] T. Yanabe, K. Yamashita, M. Kaminoyama, M. Koizumi, A. Tachibana, and K. Fukui, J. Phys. Chem. *88*, 1459 (1984).
[53] E. D. German, A. M. Kusnetsov, and R. R. Dogonadze, J. Chem. Soc. Faraday 2 *76*, 128 (1980) and references cited therein.
[54] A. M. Kuznetsov and J. Ulstrup, J. Chem. Soc. Faraday Trans. 2 *78*, 1497 (1982).
[55] P. Gross, H. Steiner, and F. Krauss, Trans. Faraday Soc. *32*, 877 (1936); J. C. Hornell and J. A. V. Butler, J. Chem. Soc. *1936*, 1361.
[56] V. Gold, Trans. Far. Soc. *56*, 255 (1960); Adv. Phys. Org. Chem. *7*, 259 (1969).
[57] A. J. Kresge, Pure Appl. Chem. *8*, 243 (1964).
[58] J. Bigeleisen, J. Chem. Phys. *23*, 2264 (1955).
[59] W. J. Albery and H. H. Limbach, J. Chem. Soc. Faraday Discuss. *24*, 291 (1982).
[60] W. J. Albery, J. Phys. Chem. *90*, 3773 (1986).
[61] A. Claisen, Lieb. Ann. Chem. *287*, 366 (1895); G. Heller, Chem. Ber. *37*, 3116 (1904).
[62] G. Schenker and K. Bösl, Pharmazie *24*, 653 (1969).
[63] N. E. White and M. Kilpatrik, J. Phys. Chem. *59*, 1044 (1955).
[64] H. U. Sieveking and W. Lüttke, Lieb. Ann. Chem. *1977*, 189.
[65] C. Carvajal, K. J. Tölle, J. Smid, and M. Swarc, J. Am. Chem. Soc. *87*, 5548 (1965); D. J. Metz and A. Glines, J. Phys. Chem. *71*, 1158 (1967).
[66] W. Marquardt, Share Distribution Center, Program No. 1428 (1964).
[67] R. Kubo, Nuovo Cimento, Suppl. *6*, 1063 (1957); R. A. Sack, Mol. Phys. *1*, 163 (1958).
[68] S. Alexander, J. Chem. Phys. *37*, 971 (1962).
[69] G. Binsch, J. Am. Chem. Soc. *91*, 1304 (1969).
[70] R. R. Ernst, G. Bodenhausen, and A. Wokaun, "Principles of Nuclear Magnetic Resonance in One and Two Dimensions." Clarendon Press, Oxford 1987.
[71] M. Goldman, J. Magn. Reson. *60*, 437 (1984).

(Eingegangen am 29. Oktober 1987) E 6641